Durham University

Durham E-Theses

Investigation of the Role of MERISTEM-DEFECTIVE (MDF) in Arabidopsis thaliana Root Development

KAKKAR, MEDHAVI

How to cite:

KAKKAR, MEDHAVI (2019) *Investigation of the Role of MERISTEM-DEFECTIVE (MDF) in Arabidopsis thaliana Root Development* , Durham theses, Durham University. Available at Durham E-Theses Online: http://etheses.dur.ac.uk/13167/

Use policy

The full-text may be used and/or reproduced, and given to third parties in any format or medium, without prior permission or charge, for personal research or study, educational, or not-for-profit purposes provided that:

- a full bibliographic reference is made to the original source
- a link is made to the metadata record in Durham E-Theses
- the full-text is not changed in any way

The full-text must not be sold in any format or medium without the formal permission of the copyright holders.

Please consult the full Durham E-Theses policy for further details.

Academic Support Office, The Palatine Centre, Durham University, Stockton Road, Durham, DH1 3LE
e-mail: e-theses.admin@durham.ac.uk Tel: +44 0191 334 6107
http://etheses.dur.ac.uk

Investigation of the Role of *MERISTEM-DEFECTIVE* (*MDF*) in *Arabidopsis thaliana* Root Development

Medhavi Kakkar

Submitted for the qualification of Master of Science (MSc)

Department of Biosciences, Durham University

March 2019

ABSTRACT

Due to their sessile nature, plants have evolved to employ a sophisticated network of genetic and hormonal signalling pathways in order to modulate their development and responses to changing environmental conditions. Understanding these mechanisms is an important objective for plant developmental biologists and crop breeders, especially in the context of food security and climate change. Plant roots present an important target for trait optimisation due to their essential role in water and nutrient uptake from the soil. This thesis focuses on the regulatory role of splicing in root growth and development.

Splicing is one of the processes involved in the generation of mature RNA, and is catalysed by a macromolecular complex known as the spliceosome. Many different components are involved in this process, potentially including the putative splicing factor gene *MERISTEM-DEFECTIVE* (*MDF*), which has been found to have a role in the organisation and maintenance of root meristems. Using *Arabidopsis thaliana*, this gene was investigated in order to further understand the underlying molecular mechanisms of root formation.

To investigate the potential function of this putative splicing factor in the catalytic activation of the spliceosome, a yeast two-hybrid screen was conducted to explore protein-protein interactions between MDF and orthologs of human and yeast proteins known to interact with their MDF counterparts. No positive interactions were identified however, potentially due to the nature of the experimental setup. Indirect MDF-dependent regulation of root meristem-related genes was also briefly addressed. Downstream targets of MDF were examined through investigation of splicing-related genes differentially expressed and mis-spliced in *mdf* mutants, with a potential link identified between one of these genes, *SR34*, and root-specific stress responses.

TABLE OF CONTENTS

LIST OF FIGURES

LIST OF TABLES

LIST OF ABBREVIATIONS

Standard abbreviations have been used for mass (ng, µg, g), volume (µl, ml, L), temperature (°C), voltage (V), amount (fmol), molarity (nM, µM, mM, M), pressure (Pa), illuminance (lux), time (s, min, h), rotational speed (rpm), length (nm, mm, cm), base pairs (bp), and resolution (dpi).

Standard nomenclature for genes and proteins is used throughout, with genes italicised and proteins non-italicised, wild type genes and proteins capitalised, and mutant forms of either in lower case.

Standard convention for naming chemical element signs and nucleic acid bases has been used throughout.

Additional abbreviations in this thesis are as follows:

3AT	3-amino-1,2,4-triazole
A	Adenine
ABA	Abscisic acid
ACT2	*ACTIN2*
AD	Activation domain
ADE2	*ADENINE2*
att	Attachment site
Auto-activation	Autonomous activation
BD	Binding domain
bp	Base pairs
cDNA	Complementary DNA
CLV3	*CLAVATA3*
Col-0	Columbia-0
DNA	Deoxyribonucleic acid
E. coli	*Escherichia coli*
EDTA	Ethylenediaminetetraacetic acid

gDNA	Genomic DNA
H	Histidine
HAT	Half-A-TPR
HIND	Hub1 interaction domain
HIS3	*HISTIDINE3*
KCl	Potassium chloride
KOH	Potassium hydroxide
L	Leucine
LB	Left border
LB agar	Luria-Bertani agar
LP	Left primer
MDF	*MERISTEM-DEFECTIVE*
$MgCl_2$	Magnesium chloride
MQ	Milli-Q
mRNA	Messenger RNA
MS	Murashige & Skoog
NaCl	Sodium chloride
NaOH	Sodium hydroxide
NASC	Nottingham Arabidopsis Stock Centre
PCR	Polymerase chain reaction
PIN	*PINFORMED*
PLT	*PLETHORA*
pre-mRNA	Precursor mRNA
QC	Quiescent centre
RdDM	RNA-directed DNA methylation pathway
RMM	RNA recognition motifs
RNA	Ribonucleic acid
RP	Right primer
RS	Arginine–serine
S. cerevisiae	*Saccharomyces cerevisiae*
SART-1	Squamous cell carcinoma-associated reactive antigen for cytotoxic T-cells
SD	Synthetic defined
sdH_2O	Sterile deionised water

SDS	Sodium dodecyl sulphate
SIGnAL	The Salk Institute Genomic Analysis Laboratory
siRNA	Small interfering RNA
snRNP	Small nuclear ribonucleoprotein particle
SOC	Super optimal broth with catabolite repression
SR	Serine–arginine
TAIR	The Arabidopsis Information Resource
T-DNA	Transfer DNA
Tm	Melting temperature
TPR	Tetratricopeptide repeat
Tris-HCl	Tris hydrochloride
tri-snRNP	Tri-small nuclear ribonucleoprotein
v/v	Volume/volume
W	Tryptophan
w/v	Weight/volume
WT	Wild type
WUS	*WUSCHEL*
Y2H	Yeast two-hybrid
YPDA	Yeast peptone dextrose adenine

STATEMENT OF AUTHORSHIP

I confirm that the research presented in this thesis is my own work unless otherwise acknowledged or referenced in the text, and that material contained in the thesis has not been previously been submitted for a degree in this or any other institution.

STATEMENT OF COPYRIGHT

"The copyright of this thesis rests with the author. No quotation from it should be published without the author's prior written consent and information derived from it should be acknowledged."

ACKNOWLEDGEMENTS

I would first and foremost like to express my very profound gratitude to Keith Lindsey for being the most supportive supervisor I could ask for. Your positivity, invaluable guidance, and, frankly, inexplicable faith in my abilities have been the reason this thesis exists. Thank you also to Jen Topping, not only for your technical expertise, but for providing me with so many fantastic opportunities outside of this masters that have only strengthened my love for science and science communication. I would also like to thank Helen Thompson, for whom I am eternally grateful. I have never met anyone as resilient, compassionate, fiercely independent, and genuine as you. Thank you for being a great colleague, collaborator, mentor, and role model.

I am forever indebted to members of Patrick Hussey's group, most notably Johan Kroon and Teresa Braga, for being so incredibly generous with their advice and resources (notably vectors) for the cloning and yeast two-hybrid sections of this thesis. Thank you Teresa for being the most patient teacher, and dear friend. Thank you so much for the laughs, for your time, and for your unconditional encouragement.

Special thanks are also due to Miguel de Lucas, Peter Etchells, and Joey Nelson, for their insight and advice concerning all things cloning and yeast. Thank you Joey, especially, for all the chats about statistics, the scientific method, and life. Thank you to Flora Hetherington and Amy Jacobsen, for making me feel immediately welcome when I joined this lab, for helping me with microscopy (i.e. reassuring me that I would not break the expensive equipment), and for becoming my dearest friends and inspirations. Thank you to Rodrigo, Xiaoyan, George, Fahad, Cian, Becca, Lauren, Luke, and everyone else who has passed through Lab 1004 and the ICBL in the time I have been here. Thank you to the members of my thesis committee, Adam Benham and Gary Sharples, for being so understanding and reassuring throughout this whole process. I would also like to thank Peter Etchells and Brendan Davies for examining this thesis and providing such insightful comments.

This list would not be complete without recognition of my favourite Doctors – Paige Panter, Fieka Sukiran, Alice Rowland, and Vanessa Longden - for their friendship, unwavering support, and infinite supply of much needed hugs. My deepest appreciation also goes to my parents, for keeping me grounded when things inevitably got too stressful or overwhelming.

Finally, I would like to thank everyone else who has made my time in this department so enjoyable during this masters (except Max), and also give my sincerest apologies to all the plants, bacteria, and yeast that were sacrificed for the sake of this thesis.

1. INTRODUCTION

Plants employ an intricate and complex network of molecular mechanisms in order to modulate tissue and organ development. An arsenal of responsive genetic and hormonal signalling pathways is crucial to ensure correct growth and development, especially in the presence of abiotic and biotic stresses. Understanding these underlying mechanisms, especially in potentially fluctuating and even unfavourable environments, is an important objective for plant developmental biologists.

1.1. PLANT ROOTS

Plant roots are fundamental to plant growth and survival due to their essential role in the perception and uptake of water and nutrients from the soil. Alongside resource acquisition, roots provide anchorage, a means of nutrient storage, and they engage in communication with the microbiota of the rhizosphere. Below-ground traits of plants, even in many crop species, are unsurprisingly less well-understood compared to their aerial counterparts, due to the difficulties associated with their observation and analysis *in situ*. Huge variability exists between the root system architecture of different species, but also within species as a result of the spatial and temporal variations they experience in their surrounding environment. The phenotypic plasticity of roots allows for adaptive growth responses that take into account changes in environmental conditions, including the availability of water and nutrients (Robinson, 1994; López-Bucio *et al.*, 2003; Bengough et al, 2011), as well as biotic and abiotic stresses (Peterson, 1992; Iyer-Pascuzzi *et al.*, 2011), all of which contributes to plant survival. Understanding root development, growth, and responses to external stimuli is essential for breeding crops with greater productivity and survivability in order to improve food security and environmental sustainability, especially in the face of climate change (Beddington, 2010).

1.1.1. *Arabidopsis thaliana - A Model for Development*

Arabidopsis thaliana has proved a useful species for many plant biologists for the past 80 years or so (Laibach, 1943), owing to its small size, short generation time, self-compatibility, natural variability, inexpensive and easy growth, and ability to produce a large number of offspring (Meyerowitz, 1989). Its small nuclear genome was the first plant genome to be

published (Arabidopsis Genome Initiative, 2000), and its diploid nature has allowed for an array of tools to be developed for genetic manipulation with relative ease (Koncz *et al.*, 1992; Martínez-Zapater & Salinas, 1998). Alongside the traits that make this simple plant a useful representative for studying molecular genetics and development in flowering plants, *Arabidopsis* roots provide a convenient model for analysis. *Arabidopsis* roots have a highly ordered structure (Figure 1.1; Dolan *et al.*, 1993) following a predictable series of developmental steps. This presents an ideal system for studying many biological processes, including cellular differentiation, patterning, and polarity. *Arabidopsis* roots are easy to visualise when grown on clear agar, which makes for straightforward imaging and trait quantification.

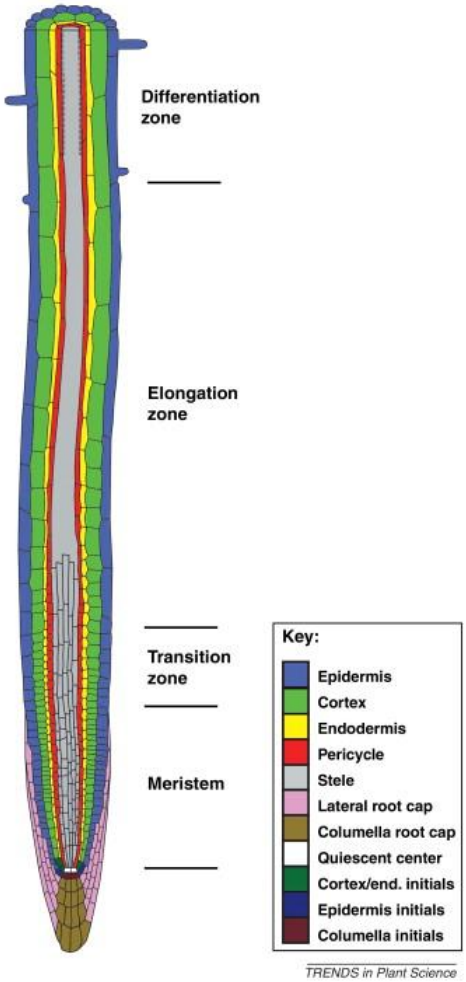

Figure 1.1. Stereotypical cellular organisation of *Arabidopsis* primary roots. Cells are arranged in single-cell files that make up concentric rings with radial organisation around a central axis. Root maturation involves distinct developmental phases through which new cells progress following their origin in the root apical meristem at the root tip. Longitudinal sectioning on the root displays its highly ordered structure, with the distinct developmental zones indicated. Figure from Ubeda-Tomás *et al.* (2012).

1.1.2. *Root Growth and Development*

When aiming to understand plant growth and survival, it is important to consider the regulation of organogenesis. During embryogenesis in higher plants, populations of undifferentiated cells, termed meristematic cells, are formed in the apices of the shoot and root, and give rise to the different cell types of the plant via a series of coordinated cell divisions (Petricka *et al.*, 2012).

At the root tip (Figure 1.2), the root apical meristem contains a group of cells with low mitotic activity, known as the quiescent centre (QC), that act as a pool of initial or stem cells. The QC provides an essential role in maintaining the undifferentiated state of these stem cell initials (Dolan *et al.*, 1993; van den Berg *et al.*, 1997; van den Berg *et al.*, 1998). The various cells of the root originate from their own specified stem cell initial through an asymmetric division that generates a daughter cell and a self-renewing cell. Repeated cell division occurs in the meristematic zone, creating longitudinally extending single-cell files. Division stops and cells begin to elongate and expand in the elongation zone, then finally specialise in the differentiation zone, all of which drives growth of the root tip into the soil (Dolan *et al.*, 1993; Beemster & Baskin, 1998; Casson & Lindsey, 2003; Verbelen et al, 2006; Petricka *et al.*, 2012; Sanz *et al.*, 2012).

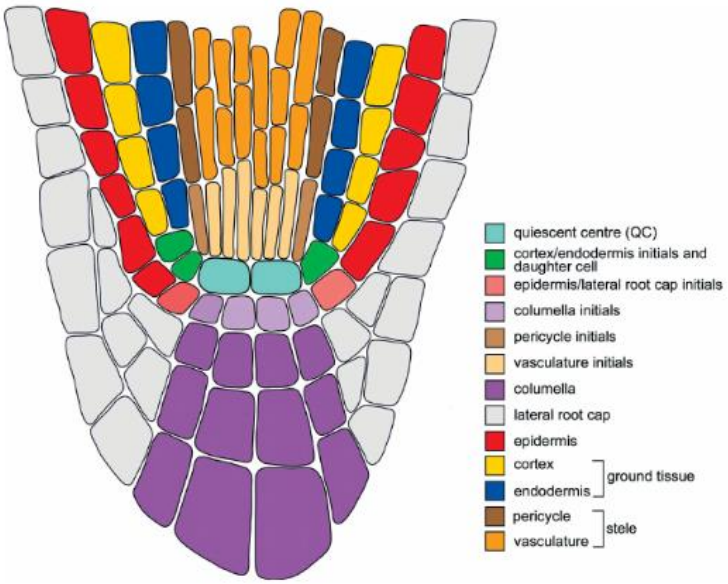

Figure 1.2. Cellular organisation of the *Arabidopsis* root meristem. The quiescent centre maintains identity of the surrounding stem cells, which divide to give rise to the various cell types (marked in different colours) of the root. Figure from Stahl & Simon (2005).

A regulated genetic program and the integration of hormonal signals underlie these tightly coordinated processes and structures (Lindsey & Topping, 1993; Petricka *et al.*, 2012; Vanstraelen & Benková, 2012; Liu *et al.*, 2014). Though many aspects of this regulation have been extensively studied, much is still left to learn about the underlying molecular mechanisms of many of the processes occurring during *Arabidopsis* root formation.

1.2. SPLICING

Regulation of RNA processing is fundamental to the development and growth of organisms (Kelemen *et al.*, 2013), and defects in splicing can result in a number of disorders (Garcia-Blanco *et al.*, 2004). Through the process of splicing, any one of a number of different variants of a protein has the potential to be produced from a single gene. Through regulation, this can be finely tuned and tailored to the needs of a particular cell or tissue type, developmental stage, and even response to environmental cues (Chen & Manley, 2009).

1.2.1. *The Spliceosome and the Splicing Process*

Splicing is one of the processes involved in the generation of mature RNA. Splicing involves the excision of intervening non-coding regions (introns) from nascent precursor messenger RNA (pre-mRNA) and the ligation of neighbouring coding sequences (exons), and is a necessary step for correct gene expression, translation, and ultimately protein biosynthesis in eukaryotes.

The catalysis of splicing involves the assembly of a multi-megadalton ribonucleoprotein complex known as the spliceosome. It is composed of small nuclear ribonucleoprotein particles (snRNPs) and non-snRNP proteins (such as ATPases, splicing factors, kinases, and helicases). Through recruitment and assembly of these various subunits, this macromolecular apparatus is able to recognise splice sites and subsequently catalyse the removal of introns from un-processed mRNA. Understanding the regulation of spliceosome activation and accurate splice site selection is an important step towards unravelling the regulatory pathways essential for the high splicing fidelity that is needed for the correct development of an organism.

The metazoan spliceosome cycle involves two coexisting spliceosome types: the major U2-dependent spliceosome, and the minor U12-dependent spliceosome. The major spliceosome acts to regulate the splicing of the majority of pre-mRNAs containing canonical (GT-AG) splice sites, and involves the so-called U1, U2, U4, U5, and U6 snRNPs (Figure 1.3). The minor spliceosome is involved in the splicing of a minority of pre-mRNAs with U12-type introns and AT-AC splice sites (Jackson, 1991; Hall & Padgett, 1994), aided by the U11, U12, U4atac, U5, and U6atac snRNPs (Hall & Padgett, 1996; Tarn & Steitz, 1996; Kolossova & Padgett, 1997).

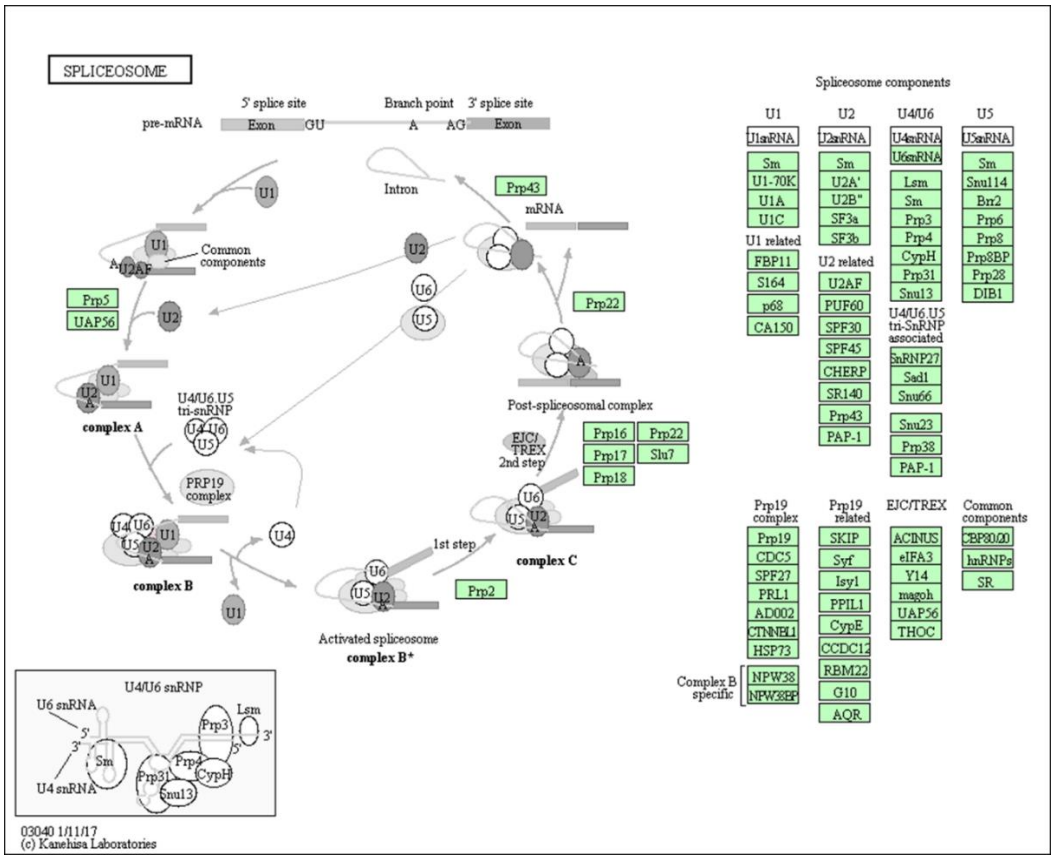

Figure 1.3. The mammalian major spliceosome cycle. Spliceosome assembly and catalysis involves small nuclear ribonucleoprotein particles and non-snRNP proteins. The major spliceosome acts to regulate the splicing of the majority of pre-mRNAs, and involves the U1, U2, U4, U5, and U6 snRNPs. In a series of RNA-RNA and RNA-protein interactions, the snRNPs and other proteins assemble onto the pre-mRNA in a stepwise, ordered fashion. After intron excision, two ligated exons are released as mRNA, the freed intron is degraded, and the snRNPs are recycled. Figure from the Kyoto Encyclopedia of Genes and Genomes database (Kanehisa & Goto, 2000; https://www.genome.jp/kegg/).

Pre-mRNA splicing is catalysed by the major spliceosome in an ordered series of steps, whereby snRNPs and other splicing factors assemble *de novo* on the pre-mRNA substrate during each cycle of splicing. Sequences known as the branch point, 5' splice site, and 3' splice site in intron-exon junctions are identified, and take part in two transesterification reactions which results in cleavage of the 5' splice site and ligation of exons. This is followed by dissociation of the resulting products and disassembly of the spliceosome for subsequent splicing of other pre-mRNAs.

1.2.2. *Alternative Splicing*

Constitutive exons refer to those that are always spliced, whereas alternative exons are only spliced under specific conditions and in response to specific signals. Alternative splicing can manifest in several forms (such as intron retention, exon skipping, or alternative splice site selection, Figure 1.4), conferring the ability of a cell to generate multiple variations of mature mRNA species from a single pre-mRNA sequence. These sequences may give rise to protein isoforms with the inclusion or exclusion of different domains, potentially altering protein function, stability, binding, signalling, or subcellular localisation (as reviewed by Stamm *et al.*, 2005). Alternative splicing can also introduce premature termination codons into mRNA, leading to the quantitative alteration of transcript levels. mRNAs harbouring these codons can be targeted for degradation through the nonsense-mediated decay pathway, which is dedicated to remove transcripts that would otherwise be translated into non- or dis-functional proteins (McGlincy & Smith, 2008).

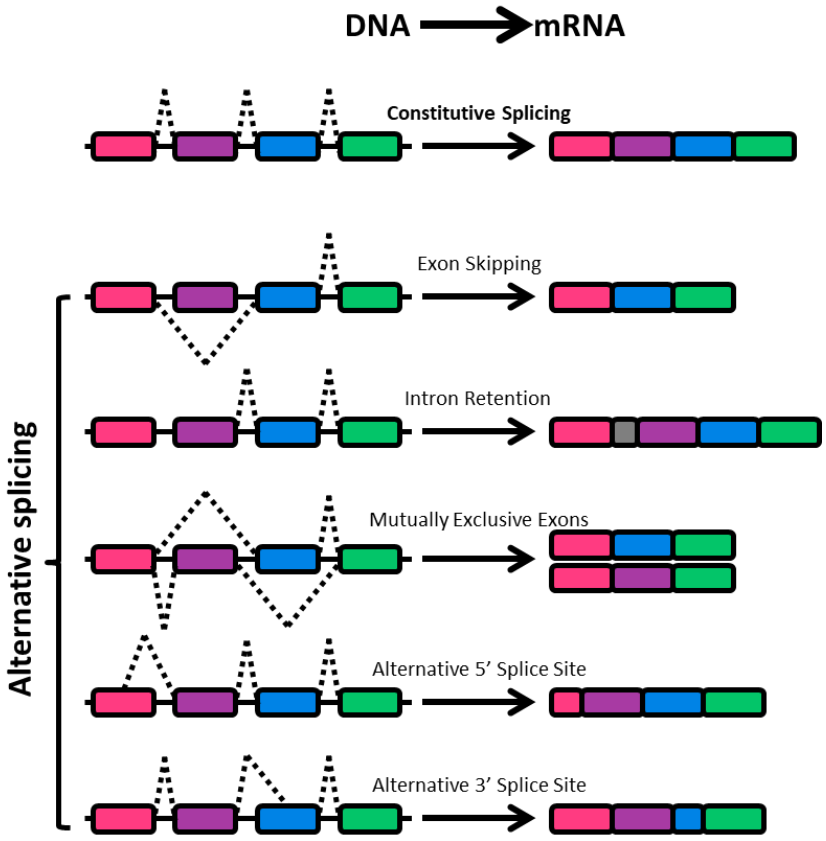

Figure 1.4. The different types of alternative splicing. The traditional classification of basic modes of alternative splicing constitutes five main types. Exon skipping refers to a splicing event where an exon may be spliced out alongside the flanking introns. Intron retention occurs when an intronic sequence is not spliced out. Mutually exclusive exons refers to the retention of one of two exons after splicing, but not both. Alternative 3' and 5' splicing events alternatively include or exclude part of an exon. Coloured boxes denote exons, solid lines represent introns, and dashed lines indicate spliced regions.

Differential regulation of splicing enables organisms to possess a vast catalogue of mRNA variants, allowing for increased coding potential and the ability to employ multiple mechanisms to control gene expression (Reddy *et al.*, 2013). For plants, this can allow for more sophisticated and efficient control over tissue and organ development, flowering time (Lee *et al.*, 2013; Posé *et al.*, 2013), the circadian clock (Seo *et al.*, 2012), and responses to biotic and abiotic stresses (Torres *et al.*, 2002; Zhang & Gassmann, 2003; Duque, 2011; Liu *et al.*, 2013; Staiger & Brown, 2013).

1.2.3. *Splicing in Plants*

A great deal is still unknown about the assembly and constituent components of plant spliceosomes, however it appears that plants possess many of the components seen in

animal spliceosomes (Lorkovic *et al.*, 2005). Much of the work conducted thus far pertains to analysis of mammalian and yeast splicing factor homologs in *Arabidopsis*, and has revealed a repertoire of splicing and spliceosome regulators much greater than that of humans (Reddy *et al.*, 2013), including greater numbers of splicing factors known as serine-arginine proteins. A better understanding of the roles of these proteins will allow for a greater appreciation of the plant—specific mechanisms involved in the regulation of splicing. Aberrant alternative splicing has been demonstrated to affect plant growth, development, and defence responses (Shad Ali *et al.*, 2007; Reddy & Shad Ali, 2011; Zhang *et al.*, 2014).

1.3. MERISTEM-DEFECTIVE

Through the regulation of processes such as transcription, splicing, and hormone signalling, embryonic and post-embryonic development of plant tissues and organs can be finely tuned, depending on factors such as cell type, location, developmental stage, and external stresses. Many different components are involved in this complex and sophisticated regulation, including the *Arabidopsis thaliana* gene *MERISTEM-DEFECTIVE* (*MDF*; *At5g16780*).

1.3.1. *Role in Maintaining Embryonic Pattering and Post-Embryonic Meristem Activity*

Using laser capture microdissection (Figure 1.5) and transcriptomic analysis of spatio-temporal gene expression patterns during embryogenesis, this gene was found to be highly expressed during the heart- and globular-stage in the basal domains of developing embryos (Casson *et al.*, 2005). GUS staining revealed relatively strong *MDF* promotor activity in the meristematic tissue of seedling shoots and roots, with particularly significant expression seen in the quiescent centre (Casson *et al.*, 2009).

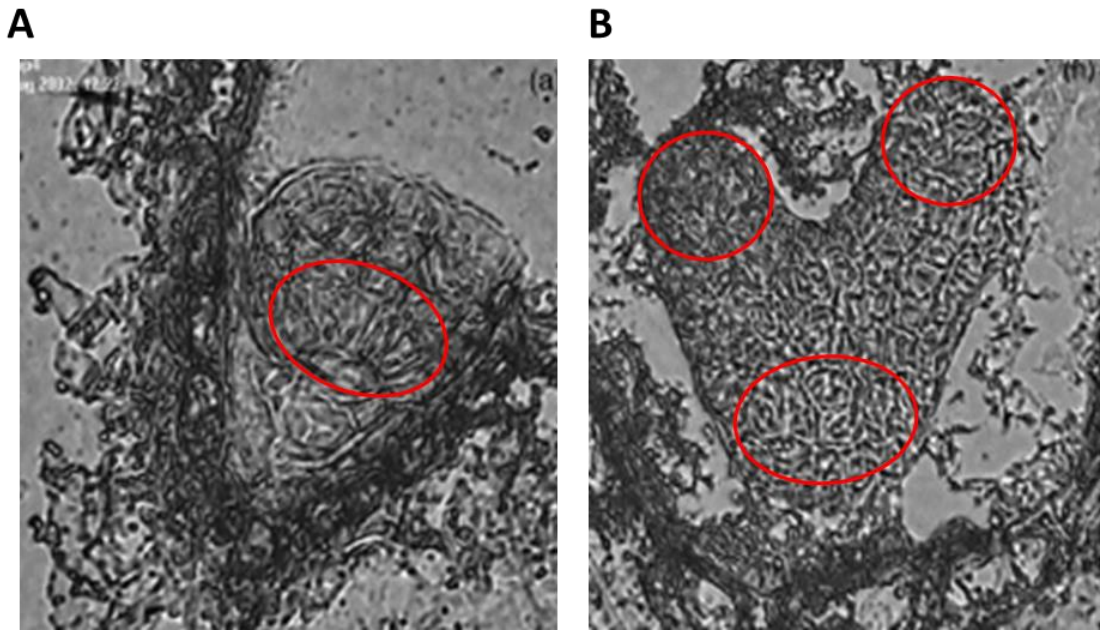

Figure 1.5. Laser capture microdissection of cryo-sections of *Arabidopsis thaliana* embryos. Red circles denote the globular- (A) and heart-stage (B) embryo cells targeted for microdissection and subjected to transcriptomic analysis by microarray. Figure adapted from Casson *et al.* (2005).

Analyses of *mdf* mutant phenotypes provided further support for the MDF protein having a crucial role in the development of roots and vegetative shoots. Individuals of the transfer-DNA (T-DNA) insertion mutant, *mdf-1* (Figure 1.6), are severely dwarfed, unable to flower, and often exhibit an aberrant number of cotyledons. Compared to wild type (WT), mutant plants have leaves with disrupted venation patterns and shorter petioles, alongside a drastic reduction in root length (Petricka *et al.*, 2008). This evidence indicating a loss of stem cell and meristematic activity in the absence of functional *MDF*, coupled with its WT gene expression pattern, supports a role for *MDF* in the organisation and maintenance of both shoot and root meristems.

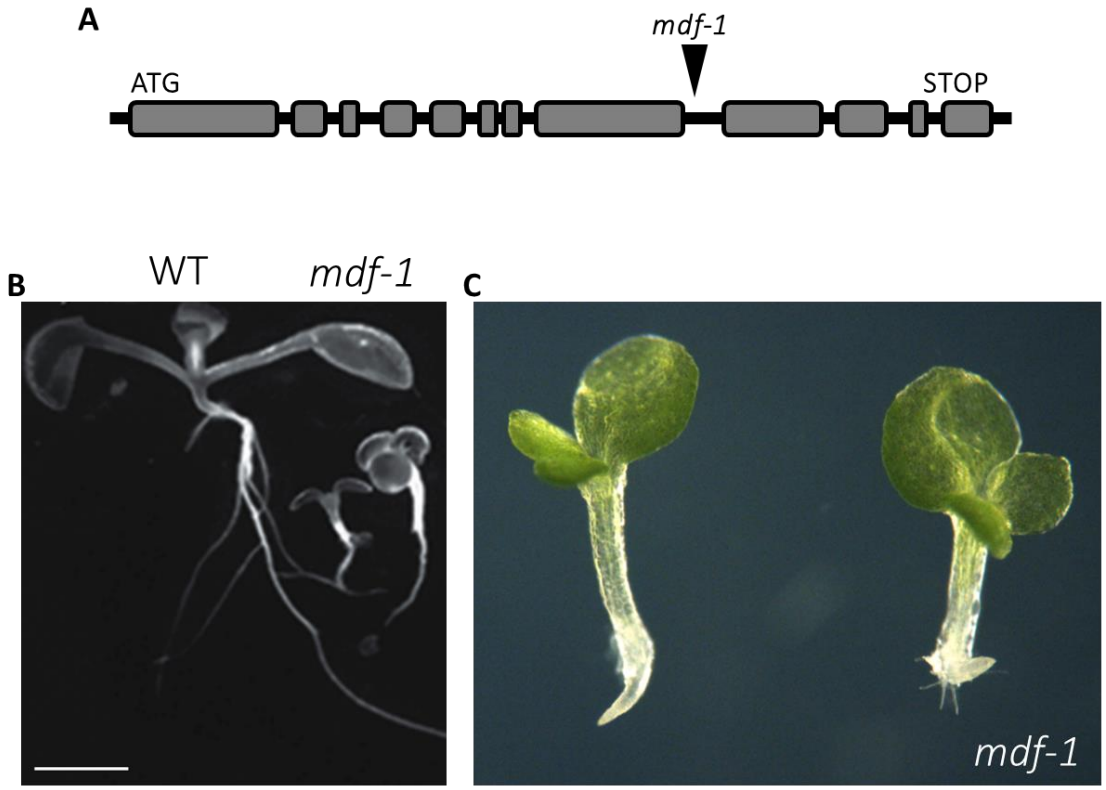

Figure 1.6. *MERISTEM-DEFECTIVE* and its mutant phenotype. (A) Schematic of the organisation of *MDF*, where boxes represent exons and solid lines represent introns. The T-DNA insertion site in *mdf-1* mutants is denoted by the solid triangle. Start (ATG) and stop codons are indicated. Figure adapted from Casson *et al.* (2009). (B) Phenotypes of wild type and *mdf-1* seedlings at 7 days post germination. The *mdf-1* mutation is lethal by 25 days post germination. Scale bar indicates 5 mm. Figure from Casson *et al.* (2009). (C) Close up of the tricotyledonous phenotype commonly seen in *mdf* mutants.

In maintaining the vegetative shoot meristem, Casson *et al.* (2009) attributes the requirement of *MDF* for the regulation of crosstalk between *WUSCHEL* (*WUS*) and *CLAVATA3* (*CLV3*) expression, both of which are regulators of stem cell population in the shoot apical meristem (Schoof *et al.*, 2000). In roots, Casson *et al.* (2009) have shown that *MDF* appears to have a role in regulating the correct expression of *PINFORMED* (*PIN*) and *PLETHORA* (*PLT*) genes, and as a result establishes proper auxin distribution, thereby aiding maintenance of meristem activity. *mdf* mutants exhibit a reduction in proximal meristem size and length of mature cells, as well as a reduction in the population of dividing cells, overall resulting in reduced root length (Figure 1.7). Since the transcription and protein levels of both PIN2 and PIN4 are also reduced in *mdf* mutants, Casson *et al.* (2009) have theorised that this has the effect of reducing the size of the proximal meristem since the expression and localisation of both proteins are important for the control of cell division in

the meristem via the auxin reflux loop (Blilou *et al.*, 2005). This results in the failure to establish and maintain the auxin maximum in the developing embryo normally critical for the formation of the seedling root meristem, leading to a reduction in *PLT* transcript levels and subsequent regulation of *PIN* gene expression (Blilou *et al.*, 2005). This ultimately disrupts patterning and maintenance of the root meristem, leading to terminal differentiation of the root meristem. *MDF* transcript levels in *plt1 plt2* double mutants remain unaffected, indicating *MDF* must act upstream of *PIN* and *PLT* gene expression. Casson *et al.* (2009) suggest that this evidence points towards *PIN* genes being likely targets of *MDF*, either through direct regulation or the regulation of other genes that modulate the expression of *PIN* genes and transcription factors associated with the meristem.

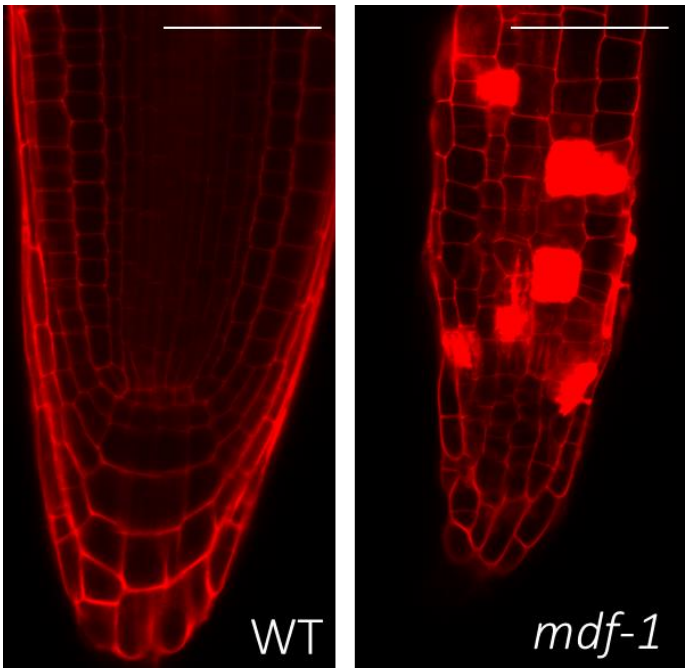

Figure 1.7. *Arabidopsis* WT and *mdf-1* roots imaged using confocal microscopy. Roots at 8 days post germination were stained using the cell wall stain propidium iodide (scale bars represent 50 µm). Disruption of root cell patterning and organisation can be observed in *mdf-1* mutants compared to WT. Shorter roots results from a reduction in the size of the proximal meristem, reduction in mature cell length, and reduction in the population of dividing cells.

1.3.2. *Structure and Homology*

MDF encodes a predicted 820-amino acid nuclear protein that shares homology to the human squamous cell carcinoma-associated reactive antigen for cytotoxic T-cells (SART-1) leucine zipper protein, with 41 % identity in the C-terminal domain (Casson *et al.*, 2009; Figure 1.8). Human *SART-1* is a gene associated with the regulation of cell proliferation,

apoptosis through cell cycle arrest (Hosokawa *et al.*, 2005), and potential transcription factor function (Gupta *et al.*, 2000; Wheatley *et al.*, 2002). SART-1, and the structurally homologous yeast protein Snu66 (Gottschalk *et al.*, 1999; Wilkinson *et al.*, 2004), make up part of the U4/U6.U5 tri-small nuclear ribonucleoprotein (tri-snRNP) complex essential for pre-mRNA processing (Gottschalk *et al.*, 1999; Stevens & Abelson, 1999; Makarova *et al.*, 2001; Makarov *et al.*, 2002). The human SART-1 protein is vital for recruiting the tri-snRNP complex to the pre-spliceosome during spliceosome assembly, most likely through mediating the interaction between U5 and U4/U6 snRNPs to form the U4/U6.U5 tri-snRNP (Makarova *et al.*, 2001; Liu *et al.*, 2006). Yeast Snu66 has also been shown to be essential for the first steps of pre-mRNA splicing *in vitro* (Gottschalk *et al.*, 1999), potentially through promoting the interaction between the tri-snRNP and the U2 snRNP. Inhibition of pre-mRNA splicing has been observed when both human SART-1 and yeast Snu66 are depleted (Gottschalk *et al.*, 1999; Makarova *et al.*, 2001; Stevens *et al.*, 2001; van Nues & Beggs 2001), signifying their necessity.

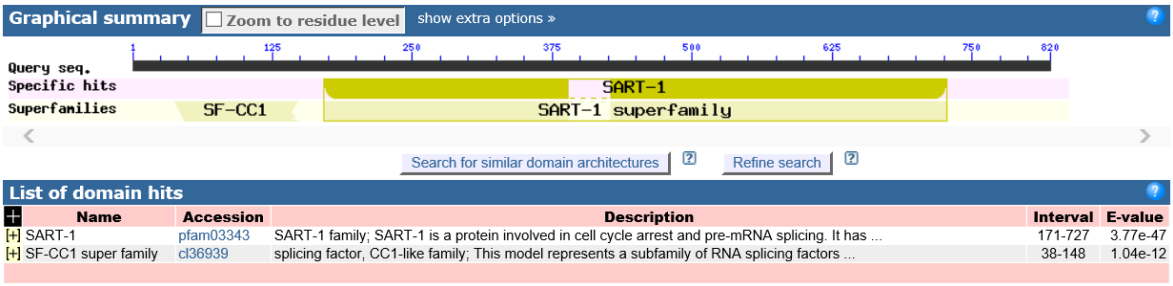

Figure 1.8. Conserved domains of MDF. MDF shares homology with the human SART-1 protein in the C-terminal region, and has an N-terminal RS domain rich in serine and arginine residues. Image generated using NCBI Conserved Domains search function (https://www.ncbi.nlm.nih.gov/Structure/cdd/wrpsb.cgi).

Both SART-1 and MDF are SR-related proteins with an N-terminus containing putative arginine–serine (RS) domains (Casson *et al.*, 2009). RS domain proteins can be broadly classified as either serine–arginine (SR) proteins or SR-related proteins. SR proteins contain one or two RNA recognition motifs (RMMs) for RNA binding specificity, and an RS domain at the C-terminus (Graveley, 2000), whereas SR-related proteins may not necessarily contain an RRM, and have different domain structures. SR proteins are vital for mature RNA formation, and act pleiotropically at various stages all the way through from the recognition of splice sites, the construction of the spliceosome, and later on down the splicing pathway. Thus far, 19 SR proteins have been identified in *Arabidopsis*, and have been shown to affect

constitutive and alternative splicing *in vivo* (Kalyna & Barta, 2004). Some of these SR proteins have been observed to undergo alternative splicing themselves (Palusa *et al.*, 2007). Current research indicates that at least nine SR and SR-related genes, alongside a whole host of other genes, are differentially spliced in *mdf-1* mutants (H Thompson, Durham University, personal communication).

SR-related proteins also have roles in spliceosome assembly, mRNA nuclear export, and transcription. RS domains in proteins such as the SR-related proteins, are rich in alternating arginine and serine residues, and are important for promoting the protein interactions needed for assembly of the spliceosome and for splice site pairing (through, for instance, binding with splicing enhancers or silencers, Wu & Maniatis, 1993; Tacke & Manley, 1999). These domains are prevalent in splicing factors. They are able to mediate interactions with other proteins that contain RS-domains, including the SR-related proteins, and have functions associated not only with constitutive and alternative pre-mRNA splicing, but also in processes such as transcription, ion homeostasis, and chromatin remodelling in animals (Boucher *et al.*, 2001). Much has yet to be learned about their biological function in plants.

With this evidence in mind, there is potential for a role for MDF in mRNA processing by mediating the assembly of splicing machinery, as well as possible other roles, such as in the regulation of meristem-related gene transcription. Understanding precisely how MDF operates to regulate, either directly or indirectly, *PIN/PLT*- and *WUS/CLV3*-mediated meristem activity requires more in-depth study. Current work being performed in this area is already providing promising results. Preliminary data (Shen, 2018) showing differential expression of genes linked to meristem development and auxin transport (including the *PIN*, *PLT*, *WUS*, and *CLV3* genes) in *mdf-1* suggests MDF is not directly responsible for the changes in expression of these genes, as they show little or no evidence of alternative splicing compared to WT. Exploring the functions and interactions of the RS and other domains of MDF may provide an insight into how this protein is necessary for correct root formation.

1.4. AIMS

The main aims of this study concerned further understanding the molecular mode of action of MDF and, more specifically, the mechanism by which MDF potentially regulates splicing through interaction with components of the spliceosome.

In order to start to unravel the link between MDF and the splicing machinery, the physical interactions between MDF and other proteins were explored. A yeast two-hybrid assay was conducted to investigate proteins that have a relationship with MDF. Potential interacting partners were selected based on orthologous interactions previously published in the literature.

The role of MDF in the direct or indirect regulation of gene expression and splicing was also investigated. Based on previous research revealing differentially expressed and spliced genes in *mdf* mutants (Shen, 2018; H Thompson, Durham University, personal communication), T-DNA insertion mutants with knock-outs of genes related to splicing regulation and the spliceosome were examined for phenotypes similar to that of *mdf*.

This project aimed to provide further evidence to support a role for *MDF* in *Arabidopsis* root development through the regulation of constitutive and alternative splicing. This research is intended to add to our overall understanding of spliceosome dynamics in *Arabidopsis thaliana*, as well as briefly tackle the regulatory pathways involved in the normal development and growth of plant roots.

2. MATERIALS AND METHODS

2.1. CHEMICALS

All solutions used in this project were prepared using autoclaved Milli-Q (MQ) water unless otherwise stated. Any solutions requiring filter sterilisation were filtered through a hydrophilic polyvinylidene fluoride membrane filter unit with a 0.22 µM pore size (Millex®), in a laminar flow cabinet. All autoclaved media and solutions were sterilised at 121 °C and 1 x 10^5 Pa for 20 mins.

The following chemicals (Sigma-Aldrich) were made up fresh (Table 2.1) and used for the stress growth assay after filter sterilisation and thorough vortexing.

Table 2.1. Chemicals used in stress assay.

Chemical	Stock Concentration (M)	Working Concentration (mM)
NaCl	2	150
Mannitol	1	300
Abscisic Acid (ABA)	0.01	0.0005

2.2. PLANT MATERIALS AND GROWTH CONDITIONS

2.2.1. *Plant Lines*

Arabidopsis thaliana plants were used in this project, with WT being of the Columbia ecotype, accession 0 (Col-0). All seeds in this project were obtained either from readily available lab stocks (WT, *mdf-1*), or The Nottingham Arabidopsis Stock Centre (NASC; http://arabidopsis.info/), with all mutant lines being in the Col-0 background (Table 2.2) unless otherwise stated. All seeds purchased from NASC were genotyped (Section 2.5.9), and only those homozygous for the T-DNA insertion were used. All splicing factor and spliceosome component mutants were selected by Dr Helen Thompson (Durham University, personal communication) based on experimental results, previous literature, and mutant availability.

Table 2.2. Details of associated loci and NASC codes for T-DNA insertion lines.

Plant Line	AGI Locus Code	NASC Code	Background
mdf-1	*AT5G16780*	SALK_040710	Col-0
sr33	*AT1G55310*	SAIL_303_F12	Col-3
sr34	*AT1G02840*	SALK_106067C	Col-0
sr45	*AT1G16610*	SALK_002537	Col-0
sr45a	*AT1G07350*	SAIL_121_B10	Col-3
rsz33	*AT2G37340*	SALK_083782	Col-0
u2.2	*AT3G57645*	SALK_131724	Col-0
u2.4	*AT3G56825*	SALK_056100	Col-0
u2.6	*AT3G56705*	SALK_023221	Col-0
u5-3	*AT1G70185*	SAIL_136_G07	Col-3
u6.29	*AT5G46315*	SAIL_1215_B04	Col-0
u12	*AT1G61275*	SALK_038216	Col-0
ubp15	*AT1G17110*	SALK_066856	Col-0

2.2.2. *Seed Sterilisation*

All seeds were surface sterilised in a laminar flow cabinet using a protocol adapted from Clarke *et al.* (1992) to prevent contamination and ensure uniform growth conditions. Seeds in 1.5 ml microcentrifuge tubes (Sarstedt) were sterilised by sequential incubation in 1 ml of 70 % v/v ethanol for 1 min (to de-wax the testa), then 10 % v/v commercial bleach with added 0.1 % v/v Tween20 (Sigma-Aldrich) as a surfactant for 15 mins. Seeds were then subjected to 4 consecutive rinse steps using sterile deionised water (sdH_2O), and finally suspended in 1 ml of sdH_2O.

2.2.3. *Plant Growth Media*

2.2.3.1. Agar

All sterilised seeds germinated on agar were surface sown onto 100 x 100 mm square Petri dishes (Sarstedt) containing half-strength Murashige and Skoog (MS; Murashige & Skoog, 2006) medium (Duchefa Biochemie) and 1 % w/v plant tissue culture grade agar (Sigma-Aldrich). Medium preparation consisted of dissolving 2.2 g of MS medium in 1 L of sdH_2O, and adjusting the pH to 5.7 using KOH. 10 g/L of agar was then added, and the solution autoclaved. Media requiring sucrose (Sigma-Aldrich) had 10 g/L of sucrose (1 % w/v) added before autoclaving. If required, solutions of the appropriate filter sterilised stress chemicals (Section 2.1) were added to media cooled to approximately 50 °C. Petri dishes were filled with 50 ml of the appropriate medium and stored at 4 °C until use. All agar plates were

stood vertically when placed inside growth chambers, with a gap of at least 10 cm between plates to reduce shade effects.

2.2.3.2. Perlite

All unsterilised seeds obtained from NASC were initially sown in a laminar flow cabinet onto perlite, a highly porous form of volcanic glass, in order to promote germination since the nature of their (potentially delicate) phenotypes was unknown. 100 x 100 mm square Petri dishes were half-filled with the substrate and soaked in autoclaved half-strength MS medium (2.2 g/L MS in sdH_2O). Excess liquid was drained from the plates and the seeds were spread onto the medium. The seeds were grown in the conditions described in Section 2.2.4, with the plates sitting horizontally in the growth chamber. The resulting seedlings were then transferred to peat for continued growth until seed production and drying, allowing for subsequent seed harvesting.

2.2.3.3. Peat

After 2 weeks of growth on perlite, all seedlings intended for growth to maturity were transferred using forceps to 44 mm re-hydrated peat plugs (Jiffy International AS), one seedling per plug. All seedlings sown onto peat were placed in trays, covered in cling film, and then transferred to a bespoke walk-in growth chamber. After 1 day ventilation holes were pierced into the film, and after another additional day in the chamber the film was removed. Plants were watered with mains water every 2 days.

2.2.4. *Growth Conditions*

After sterilisation (unless otherwise stated) and imbibition, all seeds were stratified at 4 °C for a minimum of 4 days in order to promote and synchronise germination. Seeds were then sown onto the appropriate growth medium and plates were sealed using Mircopore™ tape (3M). Plates were transferred to a 22 °C (c. 3000 lux) Versatile Environmental Test Chamber (model MLR-351; Sanyo Electric Co. Ltd.) set to long day conditions (16 h light, 8 h dark photoperiod). Any plants transferred to peat were relocated to a bespoke walk-in growth room set to the same conditions as the environmental test chambers.

2.2.5. *Root Length Measurements*

Vertical agar plates were scanned using an Epson Expression 1680 Pro flatbed scanner (Epson) at 600 dpi resolution. Primary root length was quantified from these images using the software ImageJ (Schneider *et al.*, 2012; https://imagej.net/). ImageJ data were transferred to Microsoft Excel for the production of graphs. Anchor roots were not included in analysis. Root lengths were analysed as described in Section 2.2.6.

2.2.6. *Statistical Analyses*

All statistical analyses were performed using IBM SPSS Statistics for Windows, Version 22 (IBM Corporation). An independent samples t-test was used to determine significance between the means of two independent groups at the 0.05 significance level and at a confidence level of 95 %. Although many of the datasets were not normally distributed, sample sizes were large enough for parametric statistical analyses, however due to unequal sample size and/or variance, a Welch's t-test was the test of choice.

2.3. BACTERIAL MATERIALS AND GROWTH CONDITIONS

All bacterial work needed for cloning (Section 2.7) was performed next to a roaring flame and using ethanol-flamed or otherwise sterile instruments to prevent contamination.

2.3.1. *Bacterial Strains*

Competent DH5α *Escherichia coli* (*E. coli*) cells (Invitrogen™) were used for cloning. These cells have the genotype F^- Φ80*lac*ZΔM15 Δ(*lac*ZYA-*arg*F) U169 *rec*A1 *end*A1 *hsd*R17(r_k^-, m_k^+) *pho*A *sup*E44 *thi*-1 *gyr*A96 *rel*A1 λ^-, and explanations for these genetic marker abbreviations can be found at https://www.thermofisher.com/uk/en/home/life-science/cloning/cloning-learning-center/invitrogen-school-of-molecular-biology/molecular-cloning/transformation/competent-cell-genotypes-genetic-markers.html.

2.3.2. *Bacterial Growth Media and Growth Conditions*

2.3.2.1. LB Media

Transformed *E. coli* cells were plated onto solid Luria-Bertani (LB) agar medium containing antibiotics (Section 2.3.2.3) for selection. LB agar was made up with the following components (Table 2.3), then autoclaved.

Table 2.3. Recipe for LB agar medium.

Component	**Amount (g) per 1 L of sdH_2O**
Tryptone (Melford)	5
Yeast Extract (Fisher Scientific™)	2.5
NaCl (Sigma-Aldrich)	5
Agar (Sigma-Aldrich)	7.5

Antibiotics were added to media cooled to approximately 50 °C, before 25 ml of media was poured into 90 mm diameter round Petri dishes (Sarstedt), and allowed to fully dry for at least 30 min before use. Unused plates were stored inverted at 4 °C for up to 1 month.

2.3.2.2. SOC Media

Transformed *E. coli* liquid cultures were grown up in super optimal broth with catabolite repression (SOC) medium made up with the following components (Table 2.4).

Table 2.4. Recipe for SOC medium.

Component	**Amount (g) per 1 L of sdH_2O**
Tryptone (Melford)	20
Yeast Extract (Fisher Scientific™)	5
NaCl (Sigma-Aldrich)	0.5

After mixing these components, 2.5 ml of 1 M KCl (Sigma-Aldrich) was added and the pH of the solution was adjusted to 7.0 with 10 M NaOH (Sigma-Aldrich). After autoclaving and cooling to at least 50 °C, 10 ml of filter sterilised 1 M $MgCl_2$ (Sigma-Aldrich) and 20 ml of filter sterilised 1 M glucose (Sigma-Aldrich) was added.

Antibiotics (Section 2.3.2.3) were added to the medium when required. Media without antibiotics was stored at room temperature for several months.

2.3.2.3. Antibiotics

LB agar selection plates and liquid SOC cultures contained the following antibiotics (Sigma-Aldrich) at the stated working concentrations (Table 2.5). Stock solutions were prepared in sdH_2O, filter sterilised, and stored at -20 °C in 1 ml aliquots.

Table 2.5. Antibiotic concentrations for bacterial growth media.

Antibiotic	Stock Concentration (mg/ml)	Working Concentration (µg/ml)
Gentamycin	10	10
Kanamycin	50	50
Carbenicillin	100	100

2.4. YEAST MATERIALS AND GROWTH CONDITIONS

All yeast work needed for the yeast two-hybrid assay (Section 2.8) was performed next to a roaring flame and using ethanol-flamed or otherwise sterile instruments to prevent contamination. Following autoclaving, all media was poured into 90 mm diameter round Petri dishes, and allowed to fully dry for at least 30 min before use. Unused plates were stored inverted at 4 °C for up to 1 month.

2.4.1. *Yeast Strains*

The following two *Saccharomyces cerevisiae (S. cerevisiae)* strains were used: AH109 (*MATa, trp1–901, leu2–3, 112,ura3–52, his3–200, gal4Δ, gal80Δ, LYS2::GAL1$_{UAS}$-GAL1$_{TATA}$-HIS3, GAL2$_{UAS}$-GAL2$_{TATA}$-ADE2, URA3::MEL1$_{UAS}$-MEL1$_{TATA}$-lacZ*) for bait vectors, and Y187 (*MATα, ura3-52, his3-200, ade2-101, trp1-901, leu2-3, 112, gal4Δ, met–, gal80Δ, URA3::GAL1$_{UAS}$-GAL1$_{TATA}$-lacZ*) for prey vectors. Explanations for these genotypes can be found in the Clontech Matchmaker™ GAL4 Two-Hybrid System 3 & Libraries User Manual. Both strains were kindly provided by Professor Patrick Hussey's lab group.

2.4.2. *Yeast Growth Media and Growth Conditions*

2.4.2.1. SD Media

Synthetic defined (SD) agar with 2 % glucose (Formedium) was used for to create solid media required for selecting yeast transformants and confirming auxotrophic phenotypes, and was dissolved in sdH_2O according to the manufacturer's recommendations. Amino acids are not included in the minimal base media, and were added separately in the form of dropout supplements lacking specified nutrients (Complete Supplement Mixture formulations, Formedium). Dropout solutions at 10x concentration were made up using MQ water, filter sterilised, then added to autoclaved SD agar medium (cooled to at least 50 °C) to a final concentration of 1x, or stored at 4 °C. Six types of selection media were prepared for the uses described in Table 2.6, lacking one or more of tryptophan (W), leucine (L), adenine (A), and histidine (H). Liquid SD media was prepared in the same manner, but using media lacking agar.

The use of three different types of media for the selection of protein-protein interactions through transcriptional activation of nutritional reporter genes allowed for the stringency of selection to be varied, thus helping to reduce false positives, increase the chances of detecting weak or transient, but still significant, interactions, and allowing for semi-quantitative measurement of binding affinity between interacting proteins.

Table 2.6. Dropout SD selection media and their uses in a yeast two-hybrid assay. – represents the lack of one or more nutrient.

Dropout Selection Media	Uses
–W	Select for pGBKT7 transformants
–L	Select for pGADT7 transformants
–WL	Select for pGBKT7 pGADT7 diploids Positive control for selection for interaction Low stringency test to increase the chances of detecting weak or transient interactions
–WLA	Select for protein interaction (activation of *ADE2*) Medium stringency test
–WLH with 2.5 mM 3-AT	Select for protein interaction (activation of *HIS3*) Medium stringency test
–WLAH with 2.5 mM 3-AT	Select for protein interaction (activation of *ADE2* and *HIS3* expression) High stringency test for high-affinity interactions

2.4.2.2. YPDA Media

Yeast peptone dextrose adenine (YPDA) agar medium was prepared with the following components in 1 L of sdH_2O (Table 2.7).

Table 2.7. **Recipe for YPDA agar medium.**

Component	**Amount (g) per 1 L of sdH_2O**
Peptone (Melford)	20
Yeast Extract (Fisher Scientific™)	10
Dextrose	20
Agar	16

After mixing and autoclaving of these components, 4 ml of filter sterilised adenine sulphate solution from a 10 mg/ml stock was added to 1 L of media cooled to at least 50 °C.

2.5. NUCLEIC ACID TECHNIQUES AND ANALYSES

Nuclease-free reagents and equipment, where possible, were used for all protocols involving the isolation and handling of nucleic acids, in order to minimise the risk of contamination or degradation. All surfaces and equipment were sterilised with 70 % ethanol, and nucleic acids were always handled with gloved hands to reduce exposure to nucleases. Filter tips were used for protocols requiring the extraction and handling of RNA.

2.5.1. *Quantification of Nucleic Acids*

The concentration and quality of all the RNA and DNA samples generated in this project was quantified using a NanoDrop® ND-1000 Spectrophotometer (NanoDrop Technologies LLC) following the manufacturer's recommendations.

2.5.2. *Genomic DNA Extraction*

Leaf tissue from 5 week-old plants grown on peat was used for the genotyping of T-DNA insertion lines (Section 2.5.9). Genomic DNA (gDNA) was extracted from these samples using a protocol adapted from Edwards *et al.* (1991). The lid of a 1.5 ml microcentrifuge tube was used to puncture each leaf to form leaf discs, which were flash frozen in liquid nitrogen and then ground using a sterile micropestle (Sigma-Aldrich). To each sample, 400 µl of Edward's Extraction buffer (200 mM Tris-HCl, pH 7.5; 250 mM NaCl; 25 mM EDTA;

0.5 % w/v SDS) was added, and homogenised further. After vortexing for 5 s, each tube was centrifuged for 4 min at 13000 rpm using a benchtop centrifuge, after which 300 µl of supernatant was transferred to a new tube. DNA was precipitated using 300 µl of isopropanol, with each sample inverted 3 times and left at room temperature for 2 min before centrifuging for 5 min at 13000 rpm. After discarding the supernatant, samples were mixed with 200 µl of 70 % ethanol to wash away salts, and centrifuged for 5 min at 13000 rpm. The samples were vacuum desiccated until dry using an Eppendorf concentrator 5301 (Eppendorf), and the DNA was resuspended overnight at 4 °C in 30 µl of sterile MQ water, before storage at -20 °C until use.

2.5.3. *Total RNA Extraction*

The ReliaPrep™ RNA Tissue Miniprep Kit (Promega) was used to extract total RNA from WT plant tissue samples following the manufacturer's instructions for the isolation of RNA from non-fibrous tissues. The recommended volumes of lysis solutions for ≤ 5 mg of tissue were used, regardless of the actual amount of tissue used, in order to maximise yield. Plant tissue in 1.5 ml microcentrifuge tubes was flash frozen in liquid nitrogen and stored at -80 °C until needed for extraction. The frozen tissue was ground using a micropestle prior to extraction, and further homogenised after the addition of a lysis buffer (the first step in the protocol). Isolated RNA was stored in sterile nuclease-free water (supplied in the kit) and kept at -80 °C until use.

2.5.4. *cDNA Synthesis*

The SuperScript™ IV First-Strand Synthesis System (Thermo Scientific™) was used to synthesise complementary DNA (cDNA) from RNA samples for use in cloning (Section 2.7), exploiting the greater reliability and consistency in cDNA synthesis that the SuperScript™ IV Reverse Transcriptase enzyme has to offer compared to other enzymes since high replication fidelity is needed for cloning. The manufacturer's instructions were followed, with the optional RNA removal step included. Positive control and no enzyme control reactions were conducted using supplied control cDNA. In a 20 µl reaction, 2 µg of RNA was used, and the reaction was primed with 50 µM Oligo $d(T)_{20}$.

Synthesised cDNA was checked for gDNA contamination via PCR amplification using *ACTIN2* (*ACT2*) primers (Section 2.6.1).

2.5.5. *Polymerase Chain Reaction*

All reactions involving nucleic acid sequences amplified via polymerase chain reaction (PCR) were performed using a G-storm GS1 Thermal Cycler (Gene Technologies Ltd.). Annealing temperatures for each set of primer pairs was optimised using a gradient PCR +/- 10 °C of the predicted primer melting temperatures (Tm). All PCR products were separated by gel electrophoresis (Section 2.5.6).

2.5.5.1. MyTaq™ Amplification

MyTaq™ DNA Polymerase (Bioline), and the following reaction mix (Table 2.8), was used to genotype NASC T-DNA insertion lines (Section 2.5.9), check cDNA for gDNA contamination, and screen successfully transformed bacterial colonies via colony PCR (Section 2.7).

Table 2.8. Reaction mix per 20 µl reaction for PCR amplification with MyTaq™ DNA Polymerase.

Component	**Volume in 1 x 20 µl Reaction (µl)**		
	Genotype T-DNA Insertion Lines	**Check for gDNA Contamination**	**Colony PCR**
Nuclease-free Water	14.5	14.5	9.9
5x MyTaq™ Red Reaction Buffer	4	4	4
20 µM Forward Primer	0.5	0.5	0.5
20 µM Reverse Primer	0.5	0.5	0.5
Template DNA	0.4	0.4	Single colony suspended in 5 µl of sdH_2O
MyTaq™ Red DNA Polymerase	0.1	0.1	0.1

Table 2.9 shows the cycling conditions used for each PCR reaction.

Table 2.9. Thermocycler conditions for PCR amplification with MyTaq™ DNA Polymerase.

Step	Temperature (°C)	Time (s)	Cycles
Initial Denaturation	95	60	1
Denaturation	95	15	40
Annealing	Various (Section 5)	15	
Extension	72	30	
Final Extension	72	60	1
Refrigerate	4	∞	∞

2.5.5.2. Phusion™ Amplification

Target sequences for cloning (Section 2.7) were amplified from total plant cDNA using Phusion™ High-Fidelity DNA Polymerase (Thermo Scientific™) due to its lower error rate compared to other polymerases. The following reaction mix (Table 2.10) was made up for each 50 µl reaction. Several reactions were performed with each set of primer pairs in order to obtain a sufficient amount of PCR product for use in cloning. A list of the target genes amplified can be found in Section 5. All target genes were selected by Dr Helen Thompson (Durham University, personal communication) based on literature of interactors of *MDF* homologs.

Table 2.10. Reaction mix per 50 µl reaction for PCR amplification with Phusion™ DNA Polymerase.

Component	Volume in 1 x 50 µl Reaction (µl)
Nuclease-free Water	33.5
5x Phusion HF Buffer	10
10 mM dNTPs	1
10 µM Forward Primer	1.5
10 µM Reverse Primer	1.5
Template cDNA (undiluted)	2
Phusion DNA Polymerase	0.5

The following cycling conditions were used for each PCR reaction (Table 2.11).

Table 2.11. Thermocycler conditions for PCR amplification with Phusion™ DNA Polymerase.

Step	Temperature (°C)	Time (s)	Cycles
Initial Denaturation	98	180	1
Denaturation	98	10	40
Annealing	Various (Section 5)	30	
Extension	72	120	
Final Extension	72	600	1
Refrigerate	4	∞	∞

After separation by gel electrophoresis, PCR products were purified via gel extraction.

2.5.6. *Gel Electrophoresis*

Nucleic acid samples were separated on a 1 % w/v agarose-TAE gel (1x TAE; 40 mM Tris, 20 mM Acetate, and 1 mM EDTA) pre-stained with ethidium bromide (10 µl per 100 ml of agarose-TAE). Gel tanks were connected to a PowerPac™ Basic Power Supply (BIO-RAD) set to 80 V. Nucleic acid bands were visualised using a Syngene™ InGenius LHR Gel Imaging System (Synoptics Ltd.).

For PCR products amplified using Phusion™ DNA Polymerase, 50 µl of each PCR reaction mixed with 1 µl of 5x DNA loading buffer (Bioline) was loaded per well. For samples amplified using MyTaq™ DNA Polymerase, 5 µl of PCR reaction was loaded per well. Loading buffer was not required since it was included in the supplied reaction mix. All samples were loaded alongside a separate lane containing Hyperladder™ (Bioline) of the appropriate size range.

2.5.7. *Gel Extraction of PCR Products*

The QIAquick Gel Extraction Kit (QIAGEN) was used to purify PCR products following gel electrophoresis. DNA fragments of interest were visualised on an ultraviolet transilluminator (model UVT 400-M; International Biotechnologies Inc.) and excised using a scalpel, placed in a 1.5 ml microcentrifuge tube, then recovered according to the centrifuge-based protocol described in the manufacturer's manual. Purified DNA was eluted in sterile MQ water and stored at -20 °C until needed for sequencing (Section 2.5.10) and use in cloning.

2.5.8. *Plasmid Purification*

The GeneJET Plasmid Miniprep Kit (Thermo Scientific™) was used to isolate plasmid DNA from recombinant *E. coli* cells following the manufacturer's centrifuge-based purification protocol. Plasmids were eluted in sterile MQ water and stored at -20 °C until required for sequencing (Section 2.5.10) and further use.

2.5.9. *Genotyping of NASC T-DNA Insertion Lines*

Genomic DNA was used to verify the presence of T-DNA insertions in seeds purchased from NASC. gDNA was amplified via PCR (Section 2.5.5.1) in three parallel reactions (Figure 2.1) with different combinations of the three following primers: left primer (LP), right primer (RP), and left border primer (LB). Products amplified only using the gene-specific primers, LP and RP, indicated WT DNA. These PCR products were designed to be between 900-1100 bp. If a single product of approximately 400-900 bp was amplified using one of the gene-specific primers and the T-DNA insertion-specific LB primer, then the DNA was considered to be homozygous for the insertion. Products amplified from both the LP+RP reaction as well as the LP/RP+LB reaction indicated a heterozygous genotype. These three reactions were also performed using WT DNA as a control for each set of primers. PCR products were visualised on an agarose-TAE gel.

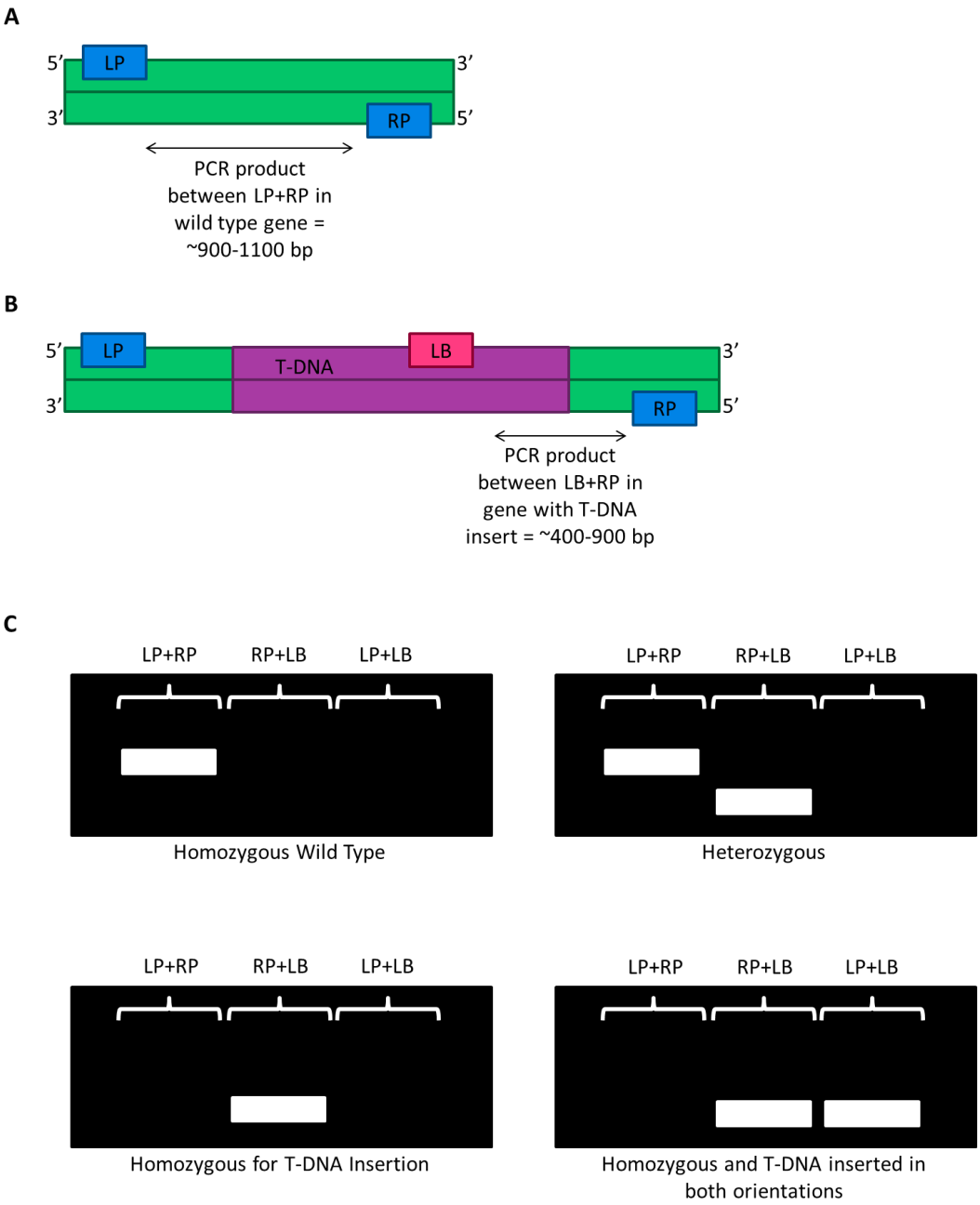

Figure 2.1. The principle of T-DNA insertion genotyping using gDNA. (A) Gene-specific primers are designed flanking the site of T-DNA insertion, but will amplify wild type DNA and produce a PCR product small enough to be visualised by gel electrophoresis. (B) The insertion-specific primer LB will produce a PCR product with RP, but the T-DNA insertion is too large for a product to be amplified with LP+RP. (C) PCR products are run on a gel and the pattern of bands indicates genotype. If the T-DNA has inserted into the gene in the opposite orientation to that stated on the SIGnAL database, then a PCR product would be produced with the LP+LB primer pair.

2.5.10. *DNA Sequencing and Sequence Analysis*

All purified PCR products and plasmids needed for cloning were sequence-verified by the DNA Sequencing Service, Department of Biosciences, Durham University.

DNA sequences were analysed using A plasmid Editor (ApE) software (http://jorgensen.biology.utah.edu/wayned/ape/) and The Arabidopsis Information Resource (TAIR) online database (https://www.arabidopsis.org/) to verify if sequences were correct. The primers used for sequencing can be found in Section 5. Any samples containing nucleotide deviations were not used.

2.6. PRIMERS

Primers were designed using gene sequences retrieved from the online TAIR database (https://www.arabidopsis.org/), and synthesised by Integrated DNA Technologies (https://eu.idtdna.com/). All primer pairs were checked using Primer-BLAST (https://www.ncbi.nlm.nih.gov/tools/primer-blast/) to ensure no non-specific or ineffective binding. A complete list of primer sequences can be found in the Appendix (Section 5).

2.6.1. *Testing Genomic DNA Contamination of cDNA*

cDNA was amplified via PCR with *ACT2* (Hetherington, 2018) primers designed to span an intron to verify if samples were contaminated with gDNA.

2.6.2. *NASC Line Genotyping PCR Primers*

Primers used to genotype T-DNA insertion lines were designed using The Salk Institute Genomic Analysis Laboratory (SIGnAL) online T-DNA Primer Design Tool (http://signal.salk.edu/tdnaprimers.2.html). The SIGnAL T-DNA database (http://signal.salk.edu/cgi-bin/tdnaexpress) was used to obtain details of the position and direction of T-DNA insertions for each mutant line.

2.6.3. *Gateway Cloning Primers*

2.6.3.1. attB PCR Primers

Cloning primers were designed to start with required Gateway® Cloning sequences in order to generate PCR products flanked with specific sequences known as *att*achment (*att*) sites.

Forward primers were designed with the following sequences to facilitate Gateway® cloning:
5’ – GGGGACAAGTTTGTACAAAAAAGCAGGCTTCGCAACA – (18-25 gene-specific nucleotides starting with start codon) – 3’

Reverse primers were designed similarly, with the following sequences:
5’ – GGGGACCACTTTGTACAAGAAAGCTGGGTC – (18-25 gene-specific nucleotides ending with stop codon) – 3’

Since no C-terminal fusion was desired, the stop codon for the gene-specific sequence was included in the reverse primer. The template-specific sequences were designed to follow conventional primer design rules, such as ending with a GC clamp, etc.

2.6.3.2. DNA Sequencing Primers

Primers used to sequence PCR products and plasmids were designed using the Eurofins Sequencing Primer Design Tool (https://www.eurofinsgenomics.eu/en/ecom/tools/sequencing-primer-design/). Multiple forward primers were designed in order to fully sequence each DNA sequence of interest, with a distance of approximately 500 bp between primers.

2.6.3.3. Colony PCR Primers

Primers for verifying successfully transformed bacterial colonies during cloning (Section 2.7) were designed using the Eurofins PCR Primer Design Tool (https://www.eurofinsgenomics.eu/en/ecom/tools/pcr-primer-design/). Primers were designed to be internal to a PCR product sequence of interest to check for successful recombination of the sequence into the desired vector. Primers were designed to be 20-25 bp in length, preferably with a 3’ GC clamp, and with a product size of approximately 500-800 bp.

2.7. GATEWAY CLONING

Using the Gateway® Cloning Technology (Invitrogen™) system, amplified cDNA sequences of target genes required for the yeast two-hybrid assay (Section 2.8) were all cloned into both pGBKT7 and pGADT7 vectors (Clontech) to facilitate their expression as bait and prey

protein constructs, respectively. Total plant cDNA from 7 day post germination WT seedlings was used to generate the initial PCR products since all the desired target transcripts would be represented.

2.7.1. *BP Reaction*

PCR products of target gene sequences amplified to contain flanking *att*B sites were used as substrates in a Gateway® BP recombination reaction with the donor vector pDONR207 in order to construct entry clones. The BP reaction was performed according to the Gateway® Technology Manual in 1.5 ml microcentrifuge tubes, with the following adjusted reaction mix (Table 2.12).

Table 2.12. Reaction mix for Gateway BP recombination reaction to generate entry clones.

Component	Volume in 1 x 5 µl Reaction (µl)
*att*B-PCR product (40 fmol)	1
pDONR207 vector (150 ng/µl, 40 fmol)	1
TE Buffer, pH 8.0	2

BP Clonase™ II enzyme mix was thawed on ice for 2 min, before being vortexed twice for 2 s. To each reaction mix, 1 µl of BP Clonase™ II enzyme mix was added and vortexed twice for 2 s, then briefly centrifuged. Reactions were incubated at 25 °C overnight, and terminated with 0.5 µl of Proteinase K solution and incubation at 37 °C for 10 mins. Entry clones were stored at -20 °C until needed for transformation.

For transformation, competent DH5α *E. coli* cells were thawed on ice for 15 mins, and 5 µl of each completed BP reaction was pipetted and mixed into 50 µl of cells. Cells were incubated on ice for 30 min, heat-shocked in a water bath set at 42 °C for 1 min, and immediately chilled on ice for 2 min. Cells were left to recover in 250 µl of pre-warmed SOC medium incubated at 37 °C for 1 hour with agitation at 200 rpm. 300 µl of each transformation was spread onto LB agar selection plates containing 10 µg/ml gentamycin, and left to incubate overnight at 37 °C. Plates with colonies were stored at 4 °C for up to 1 month.

Individual colonies were screened for successful transformation using colony PCR. Positive clones were re-streaked onto fresh selection plates which were then left to incubate at 37 °C overnight. Successful transformants were used to inoculate 8 ml aliquots of SOC medium containing 10 µg/ml gentamycin in sterile 15 ml ventilated tubes (Sarstedt), which were incubated overnight at 37 °C with shaking at 200 rpm. Glycerol stocks (0.5 ml 50 % v/v filter sterile glycerol in MQ water, 0.5 ml culture) were created from each culture, flash frozen in liquid nitrogen, and stored at -80 °C. The remaining culture was purified to isolate the entry clones (Section 2.5.8). Several cultures were grown for each construct in order to obtain a sufficient amount of plasmid. Entry clones were stored at -20 °C until needed for the LR reaction.

2.7.2. *LR Reaction*

Purified entry clones produced from the BP reaction were used as substrates in a Gateway® LR recombination reaction with the yeast two-hybrid destination vectors pGADT7 and pGBKT7 in order to generate expression clones. The LR reaction was carried out following the exact protocol as described for the BP reaction (Section 2.7.1), however with use of the following reaction mix (Table 2.13), and the addition 1 µl of LR Clonase™ II enzyme mix *in lieu* of the BP Clonase™ II enzyme mix. Instead of containing 10 µg/ml gentamycin, LB agar selection plates and SOC medium containing antibiotics used 50 µg/ml kanamycin for expression clones in the pGBKT7 vector, and 100 µg/ml carbenicillin to positively select for those in pGADT7.

Table 2.13. Reaction mix for Gateway LP recombination reaction to generate expression clones.

Component	Volume in 1 x 5 µl Reaction (µl)
Entry clone (40 fmol)	1
pGBKT7 or pGADT7 vector (150 ng/µl, 40 fmol)	1
TE Buffer, pH 8.0	2

The purified constructs were then transformed into competent yeast cells (Section 2.8).

2.8. YEAST TWO-HYBRID (Y2H)

2.8.1. *Preparation of Chemically Competent Cells and Yeast Transformation*

The Frozen-EZ Yeast Transformation II™ Kit (Zymo Research) was used to prepare competent cells using the AH109 and Y187 *S. cerevisiae* strains following the manufacturer's manual.

Competent cells were then transformed with 1 µg of each recombinant construct (Section 2.7), or empty vector, into both strains of yeast following the manufacturer's instructions (pGBKT7 constructs into Y187 and pGADT7 constructs into AH109, and also vice versa to test for interaction in the other direction). Cells were combined with the supplied transformation solution (pre-warmed in a water bath to 30 °C to improve transformation efficiency) and inverted until homogenous. The transformation mixtures were incubated in a 30 °C water bath for 1 hour rather than the suggested 45 min, and inverted several times every 15 min. 200 µl, as opposed to 50-150 µl, of the transformation mixture was spread onto growth plates until fully soaked in. Yeast transformed with pGBKT7 constructs were spread onto –W plates, and pGADT7 constructs onto –L plates, then left to incubate at 30 °C for 2-3 days. Plates with colonies were stored at 4 °C for up to 1 month or until needed for mating.

Yeast colonies successfully transformed with bait or prey vectors were used to create resuspensions in liquid SD media (containing no agar) with the appropriate –W or –L drop out. Individual colonies (three replicates per genotype) were resuspended in 3 ml of media in 15 ml sterile ventilated tubes and grown overnight at 30 °C with agitation at 200 rpm. These resuspensions were then restreaked onto –W or –L plates to make working plates, and incubated for 2 days at 30 °C. Positive control cells known to show an interaction (unpublished) were also included in this assay, and were kindly provided by Teresa Braga from Professor Patrick Hussey's lab. The remaining cultures were used to create glycerol stocks (0.5 ml 50 % v/v filter sterile glycerol in MQ water, 0.5 ml culture), which were stored at -80 °C (but not flash frozen).

From the working plates, resuspensions were made for each genotype in 200 µl of sterile MQ water, then mated to generate diploids.

2.8.2. *Mating*

Resuspensions of transformed yeast cells were used to perform matings to generate diploid cells containing two constructs destined to be tested for interaction. On YPDA plates, 5 µl of each yeast type containing the bait construct were spotted and allowed to dry (with three biological replicates per genotype from individual colonies, and three technical replicates from each colony to give the grid system shown in Figure 2.2. Then 5 µl of each yeast type containing the prey construct was spotted onto the first set of colony drops, and allowed to dry. Plates were incubated for 2 days at 30 °C. As negative controls, pGBKT7 constructs were mated against empty pGADT7, and vice versa.

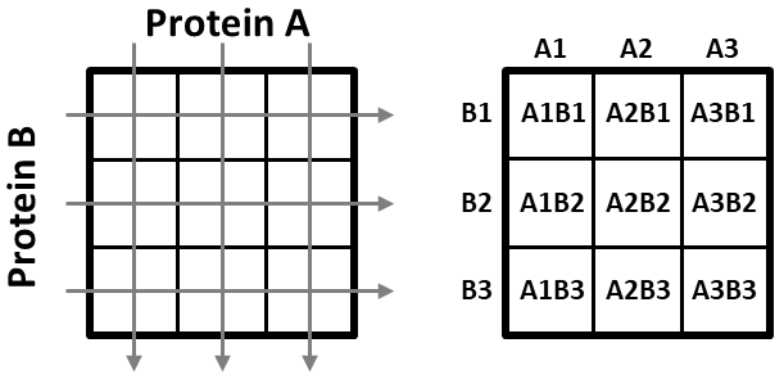

Figure 2.2. Yeast two-hybrid grid format for yeast growth plates. Three colonies of each strain of yeast were spotted in triplicate to generate biological and technical replicates. Yeast containing bait constructs (protein A) were spotted onto media and allowed to dry before yeast containing prey constructs (protein B) were spotted on top of the previous yeast. This same grid system was used for yeast mating, diploid selection, and the interaction assay. Figure adapted from Hawkins (2004).

From the mating plates, resuspensions were made from each resulting colony in 40 µl of sterile MQ water, then transferred to new plates for diploid selection.

2.8.3. *Diploid Selection*

Diploid cells were selected for by resuspending each colony of mated yeast, and spotting 10 µl of each resuspension on to –WL plates. Plates were incubated for 2 days at 30 °C.

From the interaction assay, resuspensions were made from each resulting colony in 100 µl of sterile MQ water, then transferred to new plates to select for interaction.

2.8.4. *Interaction Assay*

Resuspended diploid cells were spotted onto –WL plates as controls. For the interaction assay, diploid cells were spotted onto –WLA, –WLH with 2.5 mM 3-amino-1,2,4-triazole (3AT; Sigma-Aldrich), and –WLAH with 2.5 mM 3-AT plates. Each spot constituted 10 µl of suspension. Plates were incubated for 5-7 days at 30 °C. Haploid cells were also spotted onto each type of media as negative controls.

2.8.5. *Auto-activation Tests*

In order to remove the autonomous activation (auto-activation) of bait strains, yeast transformants for each construct mated against empty prey vectors were tested for growth on media supplemented with various concentrations of 3-AT. 3-AT is a competitive inhibitor of the *HIS3* gene product (Durfee *et al.*, 1993), and raises the minimum level of *HIS3* expression required for yeast cell survival and growth. This phenomenon is useful when selecting for high-affinity protein interactions if high concentrations of 3-AT are used, allowing for increased stringency of testing. Optimisation of 3-AT concentration is needed for control of bait-dependent reporter gene activation and resulting background growth. For this Y2H assay, 2.5 mM was selected as the optimal concentration for preventing auto-activation, and used in all selective media lacking histidine.

2.9. MICROSCOPY

2.9.1. *Light Microscopy*

Images were taken using an Olympus SZH10 stereo microscope (Olympus) equipped with a QICAM High-Performance Digital CCD Camera (Teledyne QImaging).

2.9.2. *Laser Scanning Confocal Microscopy*

For examination of cellular organisation, the cell wall stain propidium iodide (Sigma-Aldrich) was used to stain roots at a concentration of 0.5 µg/ml for 90 s. Roots were then washed in sdH_2O for 90 s, mounted onto 76 x 26 mm, 1.0 – 1.2 mm thick glass slides (Agar Scientific) with a drop of sdH_2O, covered with a 22 x 22 mm, 0.16 – 0.19 mm thick glass

coverslip (Agar Scientific), secured with nail polish, and imaged using a Leica SP5 TCS Laser Scanning Confocal Microscope (Leica Microsystems) using a x40 oil immersion objective. Excitation of propidium iodide was performed at 543 nm using the HeNe laser.

3. RESULTS

3.1. INVESTIGATING MOLECULAR INTERACTIONS BETWEEN MDF AND SPLICEOSOME COMPONENTS

MDF shares homology with proteins involved in the crucial step of spliceosome assembly whereby the U4/U6 and U5 snRNPs are recruited and tethered to yield the tri-snRNP. In order to investigate the molecular mode of action of MDF and its involvement in splicing, a yeast two-hybrid assay was conducted to test protein-protein interactions with potential interacting partners. Candidates were selected based on previous literature of known or predicted interactions of MDF homologs (Section 3.1.1). These chosen target proteins were STABILIZED1 (STA1), Pre-mRNA-processing factor 31 (PRP31), Pre-mRNA-processing factor 38 (PRP38), and ARGONAUTE 4 (AGO4). Barring AGO4, all of these targets represent U4/U6 or U5 snRNP-specific proteins.

3.1.1. *Selection of Candidate Interactors*

Selection of candidate interactors was based on several criteria. Firstly, proteins were chosen that were experimentally determined to have positive interactions with either SART-1 (the human MDF homolog) or Snu66 (the yeast MDF homolog), using at least two experimental techniques. The use of orthologous pairs to infer interologs is a common method for predicting potential protein interactions (Lee *et al.*, 2008; Nguyen *et al.*, 2013). The online protein-protein interaction databases STRING (von Mering *et al.*, 2005; https://string-db.org/) and BioGRID (Breitkreutz *et al.*, 2003; https://thebiogrid.org/) were used to search for interactions, alongside manual literature curation. Proteins were only selected if they were found to have an ortholog in *Arabidopsis thaliana*, with that ortholog having no, or few, paralogs in *Arabidopsis*. To narrow down the list of potential targets, candidates were chosen if their homologs were found have orthologous interactions in both *Saccharomyces cerevisiae* and *Homo sapiens*. Only proteins involved in spliceosome dynamics were considered. AGO4 was the exception, and chosen for the reasons described in Section 3.1.1.4. The ortholog protein nomenclature is summarised in Table 3.1.

Table 3.1. Naming conventions for protein homologs of MDF and its potential interacting partners.

Arabidopsis thaliana	*Homo sapiens*	*Saccharomyces cerevisiae*
MDF	SART-1	Snu66
STA1	PRPF6	PRP6
PRP31	PRPF31	PRP31
PRP38	PRPF38	PRP38
AGO4	AGO4	

3.1.1.1. STA1

In *Arabidopsis*, *STA1* encodes nuclear protein similar to the human U5-specific snRNP-associated splicing factor protein PRPF6, and the budding yeast splicing factor PRP6, and is implicated in the formation of the U4/U6.U5 tri-snRNP during spliceosome assembly. BLAST sequence alignment displayed 54 % identity to human PRPF6, and 28 % identity to yeast PRP6.

Full length versions of STA1 and MDF human homologs, PRPF6 and SART-1 respectively, have been observed to interact using experimental methods such as tandem affinity purification followed by mass spectrometry (Varjosalo *et al.*, 2013; Li *et al.*, 2015), and biochemical fractionation with quantitative mass spectrometry validated by independent co-fractionation experiments, affinity-purification, and functional analyses (Havugimana *et al.*, 2012; Wan *et al.*, 2015). The interaction has also been predicted, albeit weakly, using gene co-expression analysis. Gene co-expression and protein co-regulation analysis uses unsupervised machine learning (ProteomeHD; https://www.proteomehd.net) that assumes proteins differentially expressed to similar extents in response to the same biological perturbations are likely to have related cellular functions and be co-regulated. Yeast two-hybrid assays coupled with co-immunoprecipitation experiments have suggested that this interaction contributes to the establishment of contact between the two subunits of the tri-snRNP, i.e. bridging snRNP components to form the U4/U6.U5 trimer (Liu *et al.* 2006; Liu *et al.*, 2007). PRPF6 in humans is required for tri-snRNP stability, while SART-1 is not considered to do the same, despite the fact it interacts with both U4/U6 di-snRNP and U5 snRNP (Makarova *et al.*, 2001). The interaction has been hypothesised by Liu *et al.* (2006) to occur via repeats of a central HAT (Half-A-TPR) domain in PRPF6, a helical motif common to many spliceosomal proteins (Gottschalk *et al.*, 1998) that allows for binding to multiple proteins simultaneously, thereby facilitating assembly of macromolecular complexes (Scheufler *et al.*, 2000; D'Andrea & Regan, 2003). Cryo-electron

microscopy has shown that PRPF6 remodelling during B complex construction involves stabilisation by the N-terminal α-helical regions of SART-1 (Bertram *et al.*, 2017; Figure 3.1). Indeed, MDF shares structural homology with SART-1 in these helical regions, which may represent a conserved interaction domain (Figure 3.2). Bertram *et al.* (2017) suggest interaction involves SART-1 interacting with the N-terminal tetratricopeptide repeats (TPR) of PRPF6. These repeats are similar in structure and sequence to HAT motifs, and also play a role in facilitating specific protein-protein interactions, and have been predicted to be present in STA1 (using the NCBI Conserved Domains search function; https://www.ncbi.nlm.nih.gov/Structure/cdd/wrpsb.cgi). This PRPF6-SART-1 interaction may be regulated by post-translational modification, since PRPF6 is phosphorylated after incorporation into the spliceosomal B complex. It has been suggested that this could serve the purpose of modulating the function of its interacting partner, SART-1 (Schneider *et al.*, 2010). However, alternative hypotheses for the function of this phosphorylation event have also been suggested (Schneider *et al.*, 2010), such as modulating the function of other spliceosome and spliceosome-associated proteins which PRPF6 contacts during the catalytic activation of the spliceosome (e.g. PRPF31, PRPF8, BRR2, SNU114).

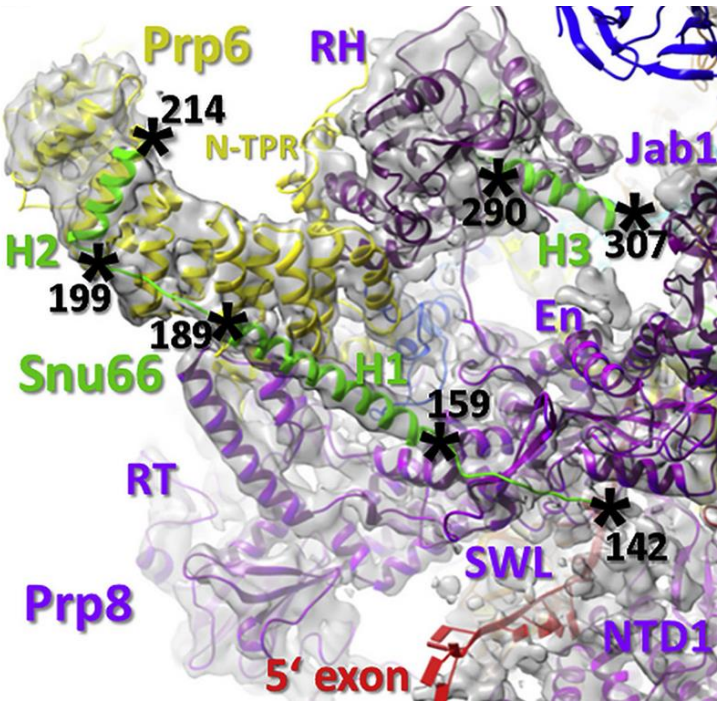

Figure 3.1. The interaction between PRPF6 and SART1. Cryo-electron microscopy reconstruction of the human spliceosome showing the stabilisation of PRPF6 (labelled Prp6) in the B complex via the N-terminal α-helices of SART-1 (labelled Snu66). Figure from Bertram *et al.* (2017).

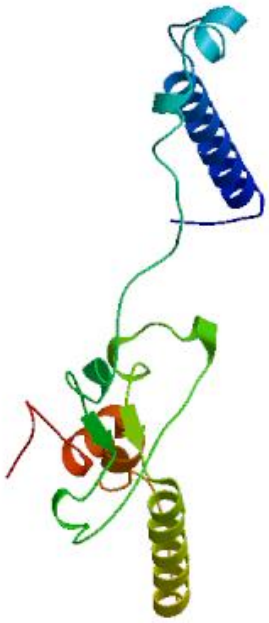

Figure 3.2. Three-dimensional homology-based model representing a predicted tertiary structure of MDF. C-terminal α-helical regions are coloured blue and yellow. Model generated using SWISS-MODEL (https://swissmodel.expasy.org/).

Similar methods have been used to show the interaction of STA1 and MDF homologs in yeast, PRP6 and Snu66, such as cryo-electron microscopy, which has demonstrated close spatial interaction of these proteins at near-atomic resolution (Plaschka *et al.*, 2017). The bridging role of the human PRPF6 protein is also seen with the yeast homolog, however, unlike in humans, yeast PRP6 does not appear to affect the integrity of the tri-snRNP (Galisson & Legrain, 1993). Previously conducted yeast two-hybrid assays have also shown an interaction between yeast PRP6 and Snu66, with the implication that Snu66 could mediate formation of the tri-snRNP through its association with PRP6 (van Nues & Beggs, 2001). This result is consistent with findings from additional protein-protein interaction experiments, including those involving tandem affinity purification (Krogan *et al.*, 2006; Mishra *et al.*, 2011).

Based on these and other observations, STA1 appears to be a prime candidate for interacting with MDF during *Arabidopsis* spliceosome assembly.

3.1.1.2. PRP31

Arabidopsis PRP31 and its orthologs encode for ubiquitous core snRNP proteins, specifically in the U4/U6 snRNP (Weidenhammer *et al.*, 1996). *Arabidopsis* PRP31 exhibits 47% identity to human PRPF31, and shares 55 % similarity and 32 % identity with yeast PRP31 (Du *et al.*, 2015). There are no paralogs of PRP31 in the *Arabidopsis* genome, with the exception of the pseudogene *AT3G60610*.

The human counterpart of PRP31, PRPF31, has a critical role in the assembly of the spliceosome (Schaffert *et al.*, 2004), specifically in the formation of the tri-snRNP (Makarova *et al.*, 2002). Human PRPF31 recruits the U4 snRNP by directly binding to its 5' region via a Nop domain (Nottrott *et al.*, 2002; Liu *et al.*, 2007), which is a motif involved in binding to RNA and proteins (Liu *et al*., 2007), and is conserved in *Arabidopsis* PRP31. Co-fractionation experiments have demonstrated an interaction between human SART-1 and PRPF31 (Havugimana *et al.*, 2012; Wan *et al.*, 2015).

The yeast ortholog, PRP31, has also been reported to be an indispensable component of the U4/U5 di-snRNP complex (Weidenhammer *et al.*, 1996) and unlike in humans, is involved in the association of the tri-snRNP with the pre-spliceosome (Weidenhammer *et al.*, 1997), or at an earlier step during tri-snRNP formation (Makarova *et al.*, 2002). an interaction between Snu66 and PRP31 has been observed using methods such as tandem-affinity-purification coupled to mass spectrometry (Gavin *et al.*, 2002; Gavin *et al.*, 2006; Krogan *et al.*, 2006), and synthetic genetic array analysis (Costanzo *et al.*, 2016).

In humans, the formation of the tri-snRNP by tethering of the U4/U6 and U5 snRNPs has been proposed to be stabilised by PRPF31 through specific interaction with PRPF6 (Makarova *et al.*, 2002; Schaffert *et al.*, 2004; Lee *et al.*, 2006; Liu *et al.*, 2006; Liu *et al.*, 2007) via the HAT/TPR repeat region of PRPF6 (Liu *et al*., 2006). Electron microscopy localisation has also mapped the yeast PRP6 and PRP31 proteins co-localising to the linker region between the U4/U6 and U5 snRNP, supporting the evidence indicating that they are bridging proteins (Schaffert *et al.*, 2004; Liu *et al.*, 2006; Häcker *et al.*, 2008).

In *Arabidopsis*, the functional association between PRP31 and STA1 has also been revealed using affinity purification and mass spectrometry (Dou *et al.*, 2013; Zhang *et al.*, 2013),

results of which were verified *in vivo* using co-immunopreciopitation and immunolocalisation techniques (Du *et al.*, 2015). It is therefore reasonable to hypothesise that *Arabidopsis* PRP31 could also associate with MDF, alongside PRP6, in order to promote stabilisation of the spliceosomal B complex during pre-mRNA splicing.

3.1.1.3. PRP38

While PRP6 is associated with the U5 snRNP, and PRP31 with the U4/U6 subunit, PRP38 is thought to be associated with the U4/U6.U5 tri-snRNP in a similar manner to SART-1. Arabidopsis PRP38 shares 65 % identity with human PRPF38, and has two regions of ~30 % identity with yeast PRP38 but limited homology elsewhere.

The human counterpart of PRP38, PRPF38, is recruited to the spliceosomal B complex stage, independent of the tri-snRNP (Agafonov *et al.*, 2011). However, in yeast, PRP38 is a stable component of the U4/U6.U5 tri-snRNP (Gottschalk *et al.*, 1999; Stevens & Abelson, 1999; Stevens *et al.*, 2001), and has a role in the dissociation of U4/U6 intermolecular helices and 5' splice site cleavage (Blanton *et al.*, 1992; Xie *et al.*, 1998). Both yeast PRP38 and human PRPF38 have been shown to interact with their MDF counterparts (Costanzo *et al.*, 2016; Schütze *et al.*, 2016).

In *Arabidopsis*, PRP38 contains putative Hub1 interaction domains (HIND) which are also present in yeast Snu66 and human SART-1, and enable protein-protein interactions with the spliceosome-associated Hub1 protein (Mishra *et al.*, 2011). Interestingly, *Arabidopsis* MDF does not contain HIND sequences, so PRP38 has been proposed to compensate for the lack of HINDs in MDF (Mishra *et al.*, 2011). Higher eukaryote PRP38 orthologs, with the exception of *S. cerevisiae*, all contain RS domains (Schütze *et al.*, 2016), which have been shown to mediate interaction with other RS-domain containing proteins. MDF contains such a domain, so perhaps PRP38 could conceivably interact with MDF via this sequence. Indeed, yeast two-hybrid screening with just the RS-containing N-terminal domain of human PRPF38 revealed binary interactions with both the tri-snRNP specific PRPF31 and SART-1 proteins (Schütze *et al.*, 2016), both of which are also recruited at the spliceosomal B complex stage. Helix α4 and the immediate surroundings within the N-terminal domain of PRPF38 are thought to represent a binding site for SART-1 (Schütze *et al.*, 2016), alongside other potential binding partners. Schütze *et al.* (2016) theorise that, at the

spliceosomal B complex stage of spliceosome assembly, both PRPF31 and SART-1 provide additional binding sites to allow for stable or efficient incorporation of PRPF38, which may act as a contact to components of the tri-snRNP.

With this evidence in mind, it would be sensible to predict that MDF may interact with *Arabidopsis* PRP38 in a similar manner to its homologs.

3.1.1.4. AGO4

AGO4 belongs to the Argonaute family of proteins, which have a role in RNA silencing processes and DNA methylation (Zilberman *et al.*, 2003; Zilberman *et al.*, 2004; Qi *et al.*, 2006). In plants, DNA methylation occurs through the RNA-directed DNA methylation pathway (RdDM), which involves small interfering RNAs (siRNAs), and the AGO4, AGO6, and AGO9 proteins (Zilberman *et al.*, 2003; Zheng *et al.*, 2007; Havecker *et al.*, 2010; Eun *et al.,* 2011). Regulation of this process has been demonstrated to involve splicing factors (Ausin *et al.*, 2012) and spliceosomal components, which have been observed to be recruited to different stages of the RdDM pathway in *Arabidopsis* (Zhang *et al.*, 2013), as well as the very similar pathway of RNAi-directed silencing in *Schizosaccharomyces pombe* (Huang & Zhu, 2014). For instance, the U5-specific STA1 appears to have a late-stage role in the RdDM pathway (Dou *et al.*, 2013), and the U4/U6-specific protein RDM16 (Huang *et al.*, 2013) is also directly involved. A functional connection has been found between PRP31 and RDM16, as well as STA1, in *Arabidopsis* transcriptional gene silencing (Du *et al.*, 2015), but no direct interaction has been observed between PRP31 and AGO4 *in vivo*. Interestingly, immunolocalisation shows that the localisation of STA1 overlaps with the localisation of AGO4 (Dou *et al.*, 2013) in Cajal bodies, distinct subnuclear foci that are the site of snRNP maturation. It has subsequently been theorised that STA1 may regulate siRNA accumulation after recruitment by an AGO4-containing effector complex (Huang & Zhu, 2014).

Given the links with STA1 and PRP31, AGO4 was therefore selected as a candidate as both these proteins have been found to interact with MDF homologs (see previous sections).

3.1.2. *Candidate Gene Isolation and Cloning*

All candidate genes were amplified by PCR with Gateway vector-compatible primers using cDNA from whole *Arabidopsis* seedlings. Full length cDNAs in the correct reading frame were used to circumvent the possibility of sub-domains of the resulting proteins interacting more strongly than full length proteins, potentially due to lack of folding restraints, and giving a false representation of the interaction. If the candidate genes had previously been screened for interaction with MDF and shown to have positive interactions, only then would shorter sequences be useful to, for instance, characterise interacting domains. PCR products resulting from amplification with Gateway primers were recombined initially into the entry vector pDONR207, and then from the entry vector into the yeast two-hybrid constructs pGBKT7 (bait) and pGADT7 (prey), which include the GAL4 transcription factor binding domain (BD) and activating domain (AD) respectively. Cloning was performed using *E. coli* cells, which when transformed with *MDF* in the pDONR207 vector showed reduced growth in terms of size and number of colonies, potentially indicative of a toxic or unstable plasmid. This, however, did not prove problematic during plasmid recovery, subsequent cloning steps, or transformation into yeast. All genes cloned successfully, with the exception of *PRP31*, which failed to amplify even after attempts with multiple annealing temperatures, cycling conditions, and reaction mixes. *PRP31* was therefore not used as a candidate interactor in this assay. Cloning of *PRP31* may have failed due to low transcript levels in the seedling samples used, however genome-wide expression data available from GENEVESTIGATOR® (Zimmermann *et al.*, 2004; https://genevestigator.com/) and the *Arabidopsis* eFP Browser (Winter *et al.*, 2007; http://www.bar.utoronto.ca/) reveal that *PRP31* is expressed at a mid-high level throughout all developmental stages and in the majority of tissues.

3.1.3. *Yeast Transformation and Yeast Two-Hybrid Assay*

The successfully cloned and sequence-verified vectors were transformed into the appropriate yeast lines, AH109 (*MATa*) for bait constructs and Y187 (*MATα*) for prey constructs. Use of different yeast mating types (with either the *a* or *α MAT* locus) allowed for the mating of haploid cells to produce diploids. Each mated yeast line displayed robust growth on –WL plates (Figure 3.3), indicating successful transformation of both bait and prey recombinant constructs and therefore respective presence of the genes required for tryptophan and leucine synthesis needed for growth on the selective media. Haploid yeast

(only able to synthesis one of tryptophan or leucine) were spotted onto the same media as negative controls, and all failed to grow.

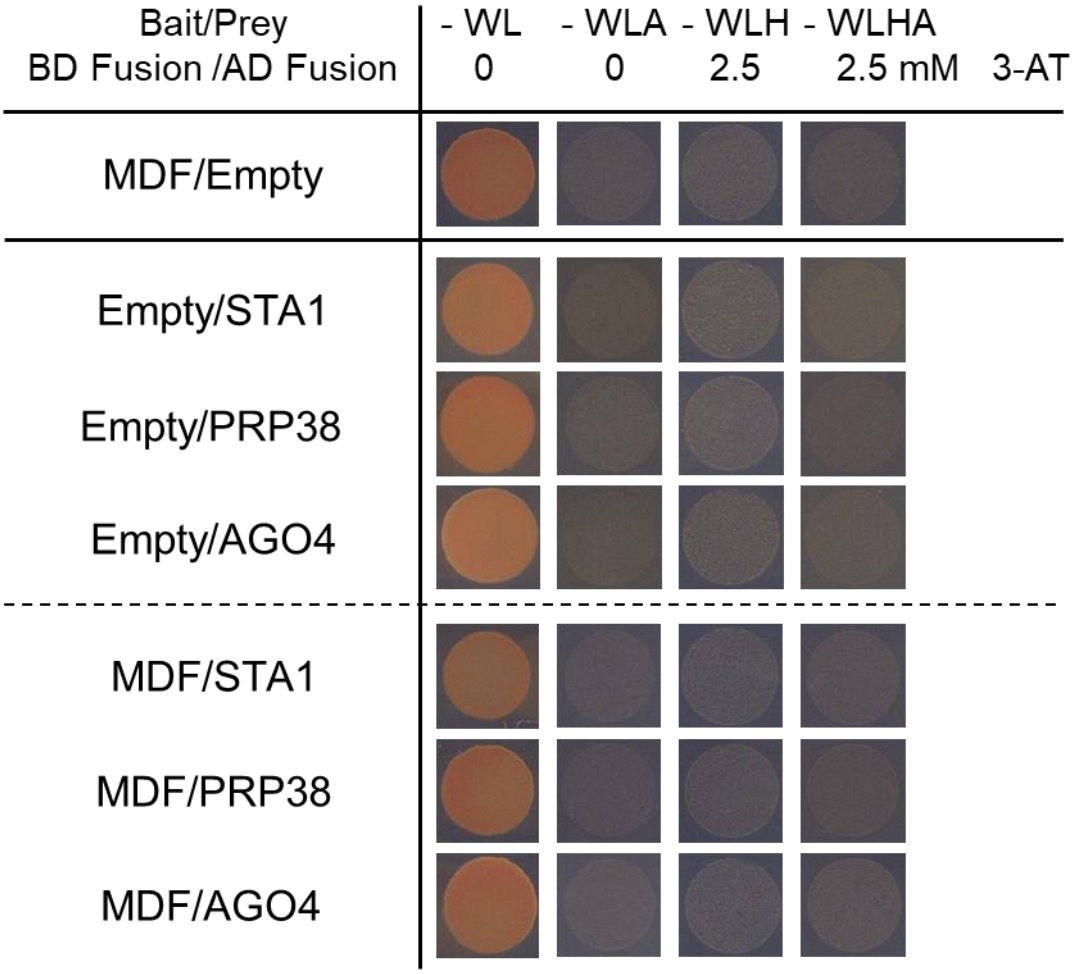

Figure 3.3. Yeast two-hybrid one-on-one tests. Full length MDF-BD fusion protein in pGBKT7 was mated against full length STA1-, PRP38- and AGO4-AD fusion proteins in pGADT7. Each recombinant construct was mated against empty vectors as negative controls. Three colonies of each yeast type were spotted in triplicate on to different selection media lacking a combination of either tryptophan (W), leucine (L), adenine (A), and/or histidine (H). One representative spot from the biological and technical replicates of each yeast strain on each type of media was chosen for this figure.

Growth on the –WLA, –WLH, and –WLAH selective media indicates a positive interaction between bait and prey. This is due to the expression of nutritional reporter genes, specifically for the synthesis of adenine, histidine, or both, with each type of media selecting for various levels of stringency for a positive interaction. In this assay, no indication of positive interactions between MDF and any of the chosen targets was found

at any level of stringency, even with MDF expressed in both the pGBKT7 (Figure 3.3) and the pGADT7 constructs (Figure 3.4) and vice versa for the candidate interactors.

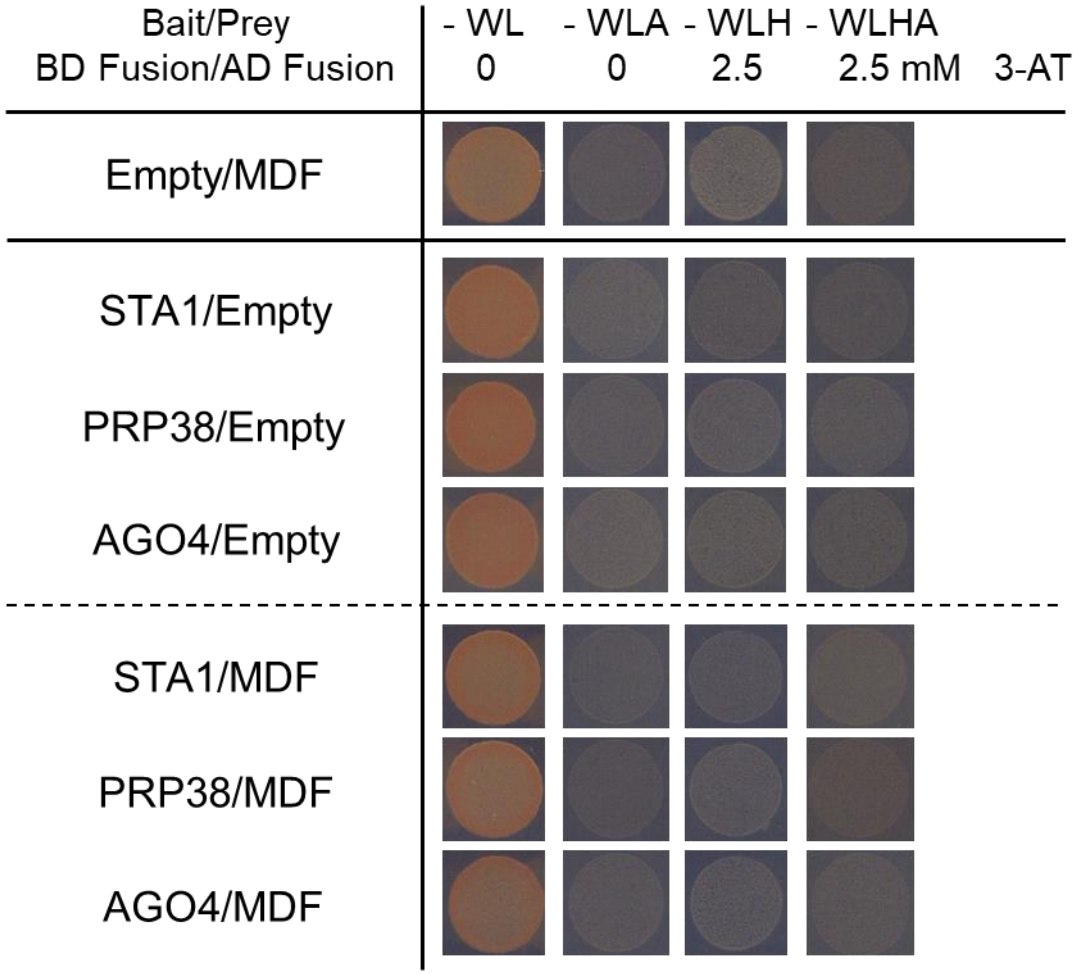

Figure 3.4. Yeast two-hybrid one-on-one reciprocal tests. Full length STA1-, PRP38- and AGO4-BD fusion proteins in pGBKT7 were mated against full length MDF-AD fusion protein in pGADT7, to test for interactions in the opposite conformation as those in Figure 3.3. Each recominant construct was mated against empty vectors as negative controls. Three colonies of each yeast type was spotted in triplicate on to different selection media to select for protein interaction at different levels of stringency. For this figure, one representative spot was chosen from the biological and technical replicates of each yeast strain on each type of media.

3.1.4. *Control and Auto-activation Tests*

Yeast expressing positive control proteins known to interact grew on each type of media, indicating the functionality of the selection media (Figure 3.5). Since there are no published interactors of MDF, no positive control could be performed to ensure that MDF expressed as a bait construct correctly folds and localises to the nucleus in yeast. Each candidate interacting protein was mated against empty vectors in order to exclude auto-activation.

Slight yeast growth was observed in several, but not all, of the replicates for the following yeast diploids on –WLH media: empty pGBKT7/STA1, empty pGBKT7/AGO4, and empty pGBKT7/MDF (Figure 3.5). Recombinant vectors containing the GAL4 AD are the commonality in this auto-activation. This residual growth could be indicative of weak, non-specific interaction, where possible nucleic acid binding domains in STA1, AGO4, and MDF bound to the *HIS3* gene, thereby bringing it in close contact with the AD domain of the pGADT7 vector and consequently activating transcription. STA1, AGO4, and MDF all contain at least one domain associated with RNA binding (i.e. HAT domain, PIWI domain, and RS domain respectively), and it is not unheard of for nucleic acid binding proteins to have non-specific affinity with other nucleic acids (Cassiday & Maher III, 2002). This explanation seems unlikely, however, since no yeast growth was observed in any other controls on any of the types of selection media. The significance of growth only on media lacking histidine and not adenine is unclear. If any positive interactions were found between the target baits and preys, the residual growth from these controls would have had to have been taken into account and would have potentially rendered the results as false positives, however since this was not the case, the interpretation of the observed results was not affected.

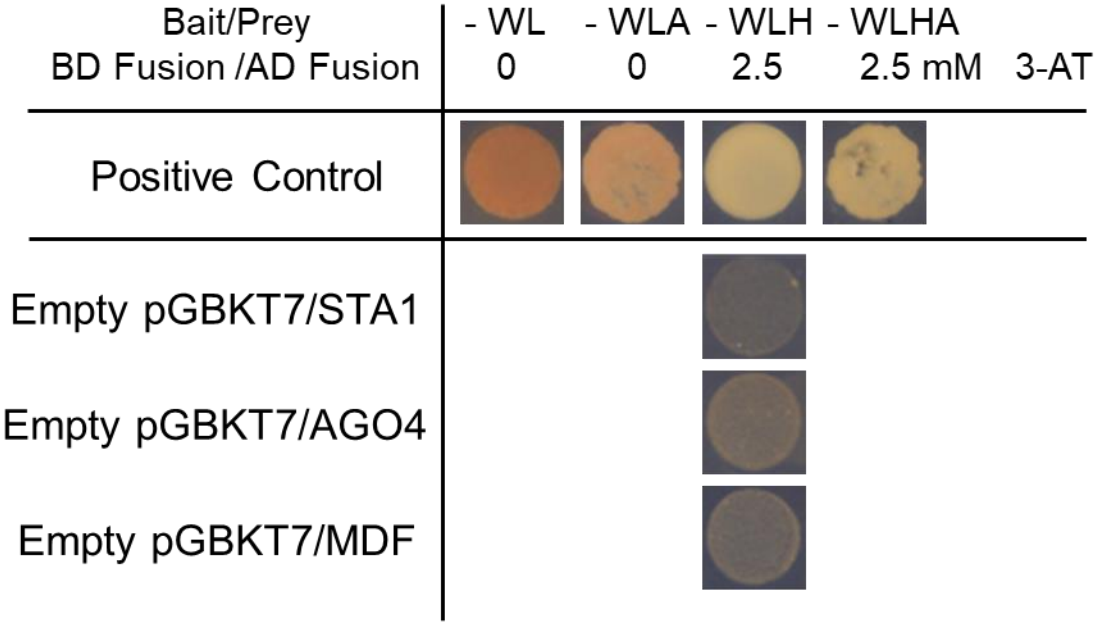

Figure 3.5. Yeast two-hybrid control tests showing auto-activation. Three colonies of each yeast type was spotted in triplicate on to different selection media. For this figure, one representative spot was chosen from the biological and technical replicates of each yeast strain.

3.2. INVESTIGATING DOWNSTREAM SPLICING FACTORS REGULATED BY *MDF*

Aside from a potential role in mediating spliceosome assembly, evidence suggests MDF plays a role in the regulation of meristem-related gene transcription (Casson *et al.*, 2009). This raises the question of how a general splicing regulator can also have such a specific additional role in *Arabidopsis*, and consequently a specific phenotype in knock-out mutants. In *mdf-1* it has been demonstrated that there is differential expression (Shen, 2018), but not differential splicing, of genes necessary for the definition and maintenance of the root meristem, such as those involved in auxin transport, stress responses, secondary metabolites, and programmed cell death (H Thompson, Durham University, personal communication). This suggests an indirect, rather than direct, role for MDF in root meristem activity. With that in mind, the next logical step in unravelling this regulatory pathway is to consider the intermediates through which MDF acts. If MDF is not directly affecting the splicing of these downstream genes, it may be regulating the splicing of other factors, such as transcription or splicing factors, which in turn affect the expression of genes involved in correct root development. MDF may also act in a splicing-independent manner to regulate root development, especially considering other SR proteins have functions such as transcription and chromatin remodelling (Boucher *et al.*, 2001). However, the previously presented evidence of homology to known splicing factors suggests a role for MDF as a regulator of splicing.

3.2.1. *Selection of Target Genes*

Unpublished analysis of alternatively spliced genes in *mdf-1* mutants (H Thompson, Durham University, personal communication) revealed a plethora of genes mis-spliced compared to WT. Since this thesis focuses on a role for MDF pertaining to the regulation of splicing, only splicing-related genes were considered (Table 3.2). Spliceosome genes differentially expressed in *mdf-1* mutants were also included (H Thompson, Durham University, personal communication), which interestingly included genes of many proteins necessary for the early stages of splicing. Only genes with *Arabidopsis* T-DNA insertion lines available from NASC were purchased, genotyped, then grown concomitantly on agar, perlite, and peat. Only those containing one T-DNA insertion and were homozygous for that insertion were considered.

Table 3.2. Splicing factors and spliceosome-related genes chosen for investigating downstream targets of MDF. Full details of associated loci and NASC codes for T-DNA insertion lines for each of these genes can be found in Table 2.2.

Description	**Gene**	**Differentially Expressed (DE) or Alternatively Spliced (AS) in *mdf-1*?**
Splicing Factors SR Proteins SF2/ASF Subfamily	*SR33*	AS – Retained intron event
	SR34	AS – Alternative 3' splice site selection and retained intron event
Splicing Factors SR Proteins SR45 Subfamily	*SR45*	AS – Retained intron event
	SR45a	AS – Skipped exon event
Splicing Factor SR Protein RS2Z Subfamily	*RSZ33*	AS – Retained intron event
Spliceosome Components Major snRNA U2 snRNAs	*U2.2*	DE – Upregulated
	U2.4	DE – Upregulated
	U2.6	DE – Upregulated
Spliceosome Component Major snRNA U5 snRNA	*U5-3*	DE – Upregulated
Spliceosome Component Major snRNA U6 snRNA	*U6.29*	DE – Upregulated
Spliceosome Components Minor snRNAs	*U12*	DE – Upregulated
	UBP15	

3.2.2. *Genotyping*

Genomic DNA extracted from leaf tissue of 5 week-old WT and mutant plants was used for genotyping. Gel electrophoresis using PCR products amplified with genotyping primers confirmed if the individuals tested were mutants homozygous for the T-DNA insertion (example of genotyping on *sr34* mutants shown in Figure 3.6). Seeds were harvested from confirmed knock-out mutants and used in further analyses.

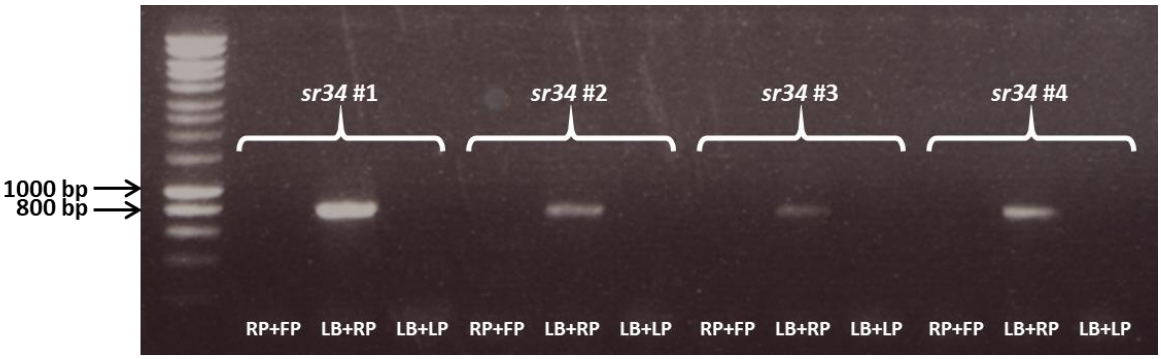

Figure 3.6. Verification of *sr34* SALK T-DNA insertion mutants. Representative tests from 4 individuals (#1-4) shown. All individuals were found to be homozygous for the T-DNA insertion since amplification was only seen with the gene-specific RP and the insertion-specific LB, with a band in the correct size range of 610-910 bp. No band was seen when both gene-specific primers, LP and RP, were used, indicating no amplification of the WT *SR34* gene. The T-DNA insertion can be assumed to be in the orientation predicted by the SIGnAL database, since no bands were present when the LP and the LB primer were used. PCR amplifications with the same 3 combinations of primer pairs were conducted using WT gDNA (not shown) as a control, where amplification was only seen with the gene-specific LP and RP primers. Hyperladder™ 1kb (Bioline) was used as the DNA size marker on the left hand side.

3.2.3. *Phenotyping*

Out of all of the mutants screened, *sr34* was found to be the most interesting candidate to pursue for further analysis. In order to ascertain whether *SR34* is involved in an MDF-dependent root development pathway, *sr34* mutants were grown vertically on clear agar in order to visualise root morphology. Sterilised seeds were sown onto half-strength MS 1 % agar medium after imbibition and stratification in the dark at 4 °C for 4 days, then transferred to a 22 °C growth chamber with a 16 h light, 8 h dark cycle for 8 days. Roots were then visualised using light microscopy. Any similarities in root phenotype to *mdf* mutants would potentially indicate a role for *SR34* downstream of *MDF*. No visual differences in root morphology (Figure 3.7) were observed between *sr34* mutants and WT seedlings.

Figure 3.7. Root morphology of WT and *sr34* plants. Plants were grown on half-strength MS agar medium and visualised using light microscopy at 4 days post germination (scale bars represent 1 mm).

Given that it has been previously demonstrated that several splicing factor mutants exhibit hypersensitivity to abiotic stress treatments (Lee *et al.*, 2006; Huang *et al.*, 2013; Du *et al.*, 2015), *sr34* mutants were subjected to a range of stress treatments and primary root length was assessed (Figure 3.8). After stratification, imbibed and sterilised WT and *sr34* seeds were sown on half-strength MS 1 % agar medium supplemented with either sodium chloride (NaCl), mannitol, abscisic acid, or sucrose, and grown vertically in a 22 °C growth chamber under long day conditions for 7 days. Concentrations for each of these medium supplements was chosen based on the concentrations Du *et al.* (2015) found to have a significant effect on the germination rate of the *Arabidopsis* splicing factor mutants *prp31*, *zop1*, and *sta1*. Under the control condition, WT and *sr34* seedlings exhibited no discernable difference in primary root length. A similar result was seen with seedlings exposed to 150 mM NaCl. However, root lengths were signicantly reduced when seedlings were grown on media supplemented with 300 mM mannitol, 0.5 µM ABA, and 1 % sucrose, indicating that *sr34* mutants are more sensitve than WT to these specific conditions.

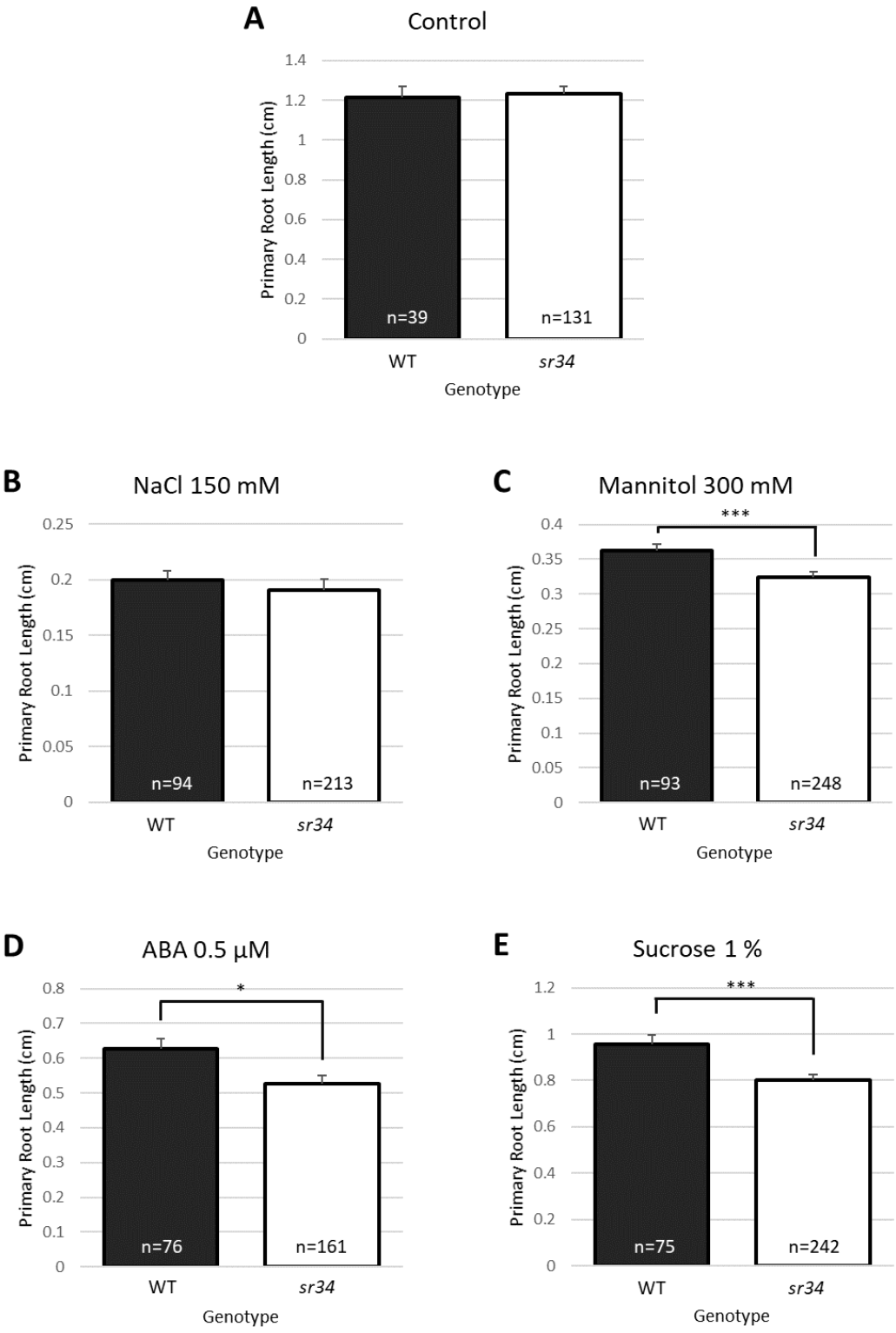

Figure 3.8. Primary root lengths of WT and *sr34* mutants grown vertically on half-strength MS agar medium with different supplements. Plates were scanned 7 days post germination and roots lengths were measured using ImageJ. Root length values are means of the sample sizes indicated, with the sample sizes reflecting three pooled biological replicates. Error bars represent ±1 standard error. Asterisks denote values with statistical difference, indicating *p* values < 0.05 (*), < 0.01 (**), or < 0.001 (***).

Mutants purchased from NASC were also sown unsterilised onto perlite hydrated with half-strength MS liquid medium, stratified in the dark at 4 °C for 4 days, then relocated to a growth chamber set to a 16 h photoperiod at 22 °C for 2 weeks. Seedlings were then transferred onto peat plugs for 5 weeks, and differences in appearance were observed. The majority of mutants displayed no qualitative differences in phenotype compared to WT, with the exception of *sr34*. When grown on peat, *sr34* seedlings were visibly smaller, paler, and more yellow than WT (Figure 3.9A). When transferred over to peat plugs and left to grow for 5 weeks, *sr34* plants displayed non-uniform growth compared to WT (Figure 3.9B). Qualitatively, variation in rosette size, petiole length, leaf shape, and survival was observed, even when the experiment was repeated using seeds collected from the individuals shown in Figure 3.9B.

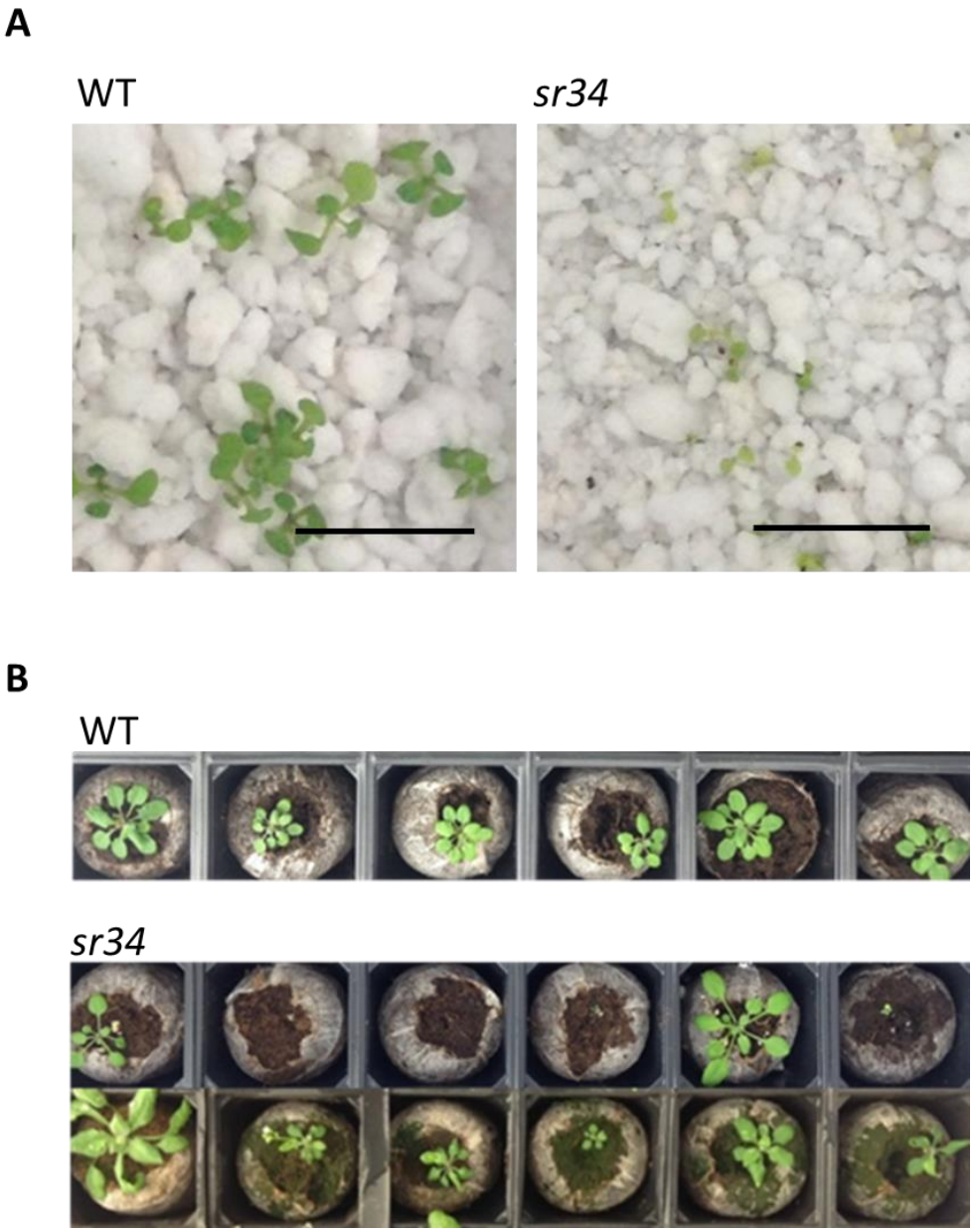

Figure 3.9. WT and *sr34* plants grown on perlite and peat. Plants were grown on (A) perlite supplemented with half-strength MS medium for 9 days, then transferred to (B) peat plugs for 5 weeks after 2 weeks growth on perlite. Scale bars represent 1 cm.

4. DISCUSSION

4.1. INVESTIGATING MOLECULAR INTERACTIONS BETWEEN MDF AND SPLICEOSOME COMPONENTS

Thus far, the components of the spliceosome have extensively been studied in mammalian and yeast systems. *Arabidopsis* spliceosomal constituents and their interactions, however, have not been as well characterised. This project, therefore, set out to gain more insight into the function of one of these components, MERISTEM-DEFECTIVE.

In order to investigate the role of MDF in the catalytic activation of the *Arabidopsis* spliceosome, a yeast two-hybrid assay was carried out to find potential binding targets. Target proteins were chosen based on known interactions of MDF orthologs from multiple species, yet no positive interactions were detected using this particular experimental technique. One of two explanations could account for this. The first is that the interaction is a true negative, and that in *Arabidopsis* MDF does not interact with STA1, PRP38, or AGO4 *in planta*, and that the interactions seen with homologs is not conserved evolutionarily. The second is that these results are false negatives, and are potentially the result of the limitations of the experimental setup. AGO4, however, was chosen as a candidate before electron microscopy imaging of a pre-catalytic human spliceosome was published (Bertram *et al.*, 2017) and revealed no link between AGO4 and spliceosome assembly. Therefore AGO4 was considered a tentative negative control, with the lack of interaction detected being unsurprising.

Given the fact that in both yeast and humans, orthologs of the candidate prey proteins, STA1 and PRP38, interact with their respective MDF homolog, it is surprising that no interaction was found with the *Arabidopsis* counterparts. The majority of core spliceosomal components are conserved in *Arabidopsis* (Wang & Brendel, 2004), with similar physiological functions and interactions for many of these proteins shared between species. Indeed, this has proven to be the case for many of the currently characterised snRNP constituents. It is, however, feasible for MDF to have an alternative role in splicing since homologs of some spliceosome components and splicing factors have different roles compared to their orthologous equivalents (Richardson *et al.*, 2011). This could account for

the results seen in this assay, if indeed they were true negative results. Finding possible interacting partners for MDF would then pose a more difficult challenge, which could be circumvented by performing a similar Y2H assay which utilises a random cDNA library to screen for interaction partners rather than performing pairwise matings of defined bait and prey proteins. A screen such as this could also prove useful in finding downstream protein targets of MDF not related to spliceosome assembly, and may provide insight into potential other functions, such as its involvement in root meristem maintenance and organisation. Other screening techniques investigating protein-protein interactions would also shed light on the role of MDF, such as tandem affinity purification coupled to mass spectrometry, or pull-down assays. Any potential positive interactions could then be validated using one-on-one methods such as co-immunoprecipitation, fluorescence resonance energy transfer and fluorescence-lifetime imaging microscopy, bimolecular fluorescence complementation, etc.

The results observed could have also been due to positive interactions failing to be detected in the specific conditions of the assay. Both the negative and positive controls indicated no reason to assume the experiment was performed incorrectly, however, false negatives from a Y2H assay could still arise due to a number of reasons (as reviewed in Brückner *et al.*, 2009; Rajagopala & Uetz, 2009). To ascertain whether the results seen were true negatives, it would have been beneficial to verify if the fusion proteins were expressed successfully in yeast. This could have been assessed by, for example, probing extracts from each yeast strain in a western blot, either using a GAL4-specific, or a bait- or prey-gene-specific, antibody. If there were detrimental effects of the fusion proteins on yeast cells however, then there may have been selection for individuals not expressing the protein. Even if the fusion proteins were successfully expressed and posed no toxicity to the cell, it is possible that, due to reasons such as steric hindrance or folding restraints, the BD and AD could be placed in a spatial configuration unsuitable for physical interaction and the formation of a functional transcription-activating unit. The importance of the orientation of protein partners within a Y2H system has been demonstrated by authors such as Burbulis & Winkel-Shirley (1999), who identified specific interactions among enzymes of flavonoid biosynthesis with their bait protein expressed as a BD-fusion, but not as an AD-fusion, potentially due to occlusion of binding sites by the GAL4 activating domain. However, reciprocal interactions were tested in the Y2H in this project with no positive interactions

detected, potentially indicating an alternative reason for the result. Differences in the expression levels of the constructs could also account for the results seen. The reason may also be due to the fact that interactions of fusion proteins in non-native yeast conditions may not reflect their true functional interactions in their endogenous environment. This could be due to potential differences in factors such as protein folding, three-dimensional structure, expression, affinity, stability, or failure to localise to the yeast nucleus (for example, as seen in van Aelst *et al.*, 1993). A two-hybrid system has been developed using *Arabidopsis thaliana* protoplasts rather than yeast, allowing for the study of *Arabidopsis* protein-protein interactions in their native context (Ehlert *et al.*, 2006), and may mitigate some of the aforementioned problems. The potential for endogenous yeast orthologs of MDF interactors to competitively bind to MDF-containing bait constructs may also be a reason for misleading results (for example, as described in Vignols *et al.*, 2005). Negating this would necessitate the use of, for example, a host yeast strain that is a knock-out for the native ortholog of the prey being tested. This, however, would not account for other unknown orthologous proteins within the yeast being sufficiently homologous to bind to MDF and able to compete with the foreign bait. It is also possible that certain post-translational modifications, such as phosphorylation, glycosylation, or formation of disulphide bonds, necessary for protein-protein interaction in higher eukaryotes are absent or occur unsuitably when in the yeast host. To address this, it is possible to co-express any modifying enzymes in yeast alongside the test proteins by introduction of a third plasmid, which has, for example, been used to successfully detect tyrosine-phosphorylation dependent interactions (Osborne *et al.*, 1996). This use of a so-called yeast tribrid, or three-hybrid, system (Osborne *et al.*, 1995), however, would require prior knowledge of the necessary third interactor. This yeast three-hybrid principle can be applied to bridging proteins as well as modifying enzymes, to investigate whether another protein is required if two proteins do not directly interact. It is even possible to add in a cDNA prey library to find a third interactor. Indeed, this system may prove more enlightening since MDF homologs have been shown to bind several proteins during spliceosome assembly, suggesting that more than two proteins could be required for an interaction to occur. Candidates for a third protein would include PRP8 (Gavin *et al.*, 2002; Gavin *et al.*, 2006; Krogan *et al.*, 2006; Hein *et al.*, 2015; Wan *et al.*, 2015; Bertram *et al.*, 2017), BRR2 (van Nues & Beggs, 2001; Gavin *et al.*, 2006; Krogan *et al.*, 2006; Liu *et al.*, 2006), and PRP4 (Gavin *et al.*, 2002; Gavin *et al.*, 2006; Hein *et al.*, 2015; Wan *et al.*, 2015), as well as various

combinations of the candidates used in this investigation (e.g. STA1 and PRP31, PRP31 and PRP38). While the assay conducted in this thesis may not have revealed any definitive interactors of MDF, there is potential for gaining more insightful results using the same methodology with some additional alterations.

4.2. INVESTIGATING DOWNSTREAM SPLICING FACTORS REGULATED BY *MDF*

Potential upstream regulators of genes differentially expressed in *mdf-1* mutants were also investigated in order to further characterise the function of MDF in root development. Previous data have revealed significant differences in the number of alternative splicing events in plants with aberrant *MDF* expression (H Thompson, Durham University, personal communication), indicating widespread mis-regulation of splicing that could be indirectly responsible for the *mdf* mutant phenotype. In *mdf-1* mutants, one such factor, *SR34*, exhibits an increased level of transcripts with a particular retained intron event, and a reduced abundance of transcripts with an alternative 3' splice site selection event (H Thompson, Durham University, personal communication). *sr34* mutants were therefore investigated to help decipher the relationship between SR34 and MDF-mediated root development.

SR34 is a general splicing factor with at least seven different splice isoforms, resulting in protein variants differing in their RS domain (Lopato *et al.*, 1999). SR34 is highly expressed in root meristem and shoots during early development and vegetative growth (Lopato *et al.*, 1999; Stankovic *et al.*, 2016), and plays an active role in many post-splicing processes, including the export, stability, and translation of mRNA. In the *sr34* knock-out line used, the site of the T-DNA insertion is present in the RS domain (Figure 4.1), which is necessary for protein-protein and protein-RNA interactions. Site-directed mutagenesis of this domain has been shown to suppress the nuclear accumulation of SR34 and decrease protein stability (Stankovic *et al.*, 2016).

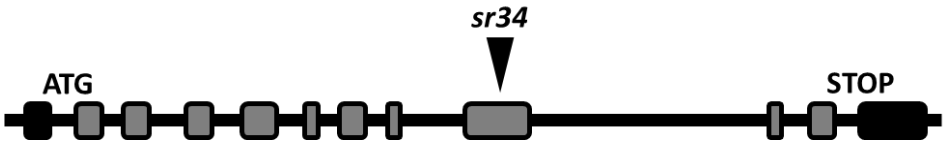

Figure 4.1. Schematic of the organisation of *SR34*. Grey boxes represent exons, solid lines represent introns, and black boxes represent untranslated regions. The T-DNA insertion site in *sr34* mutants is denoted by the solid triangle. Start (ATG) and stop codons are indicated.

When grown in standard culture conditions, *sr34* plants did not exhibit any morphological alterations, in either growth or root phenotype, compared to WT. Considering the importance of SR34 in such a ubiquitous process, an effect on growth or survival would have been expected. Functional redundancy may account for these findings. Previous studies have found that single and quadruple mutants in the SF2/ASF-like subfamily of SR proteins (Lopato *et al.*, 1996; Lorković & Barta, 2002), which consists of SR30, SR34, SR34a, and SR34b, displayed no visible phenotypes when grown on MS 0.8 % agar 1 % sucrose medium under long day conditions. These results, alongside similar findings for multiple mutants of other subfamilies, indicate potential redundancy in the functions of members of the same subfamilies of SR proteins (Yan *et al.*, 2017). These paralogous proteins have arisen through a series of gene duplication events (Simillion *et al.*, 2002; Kalyna & Barta, 2004), and consequently have high homology at the protein level with much evidence of complementary expression patterns and colocalisation. Separate, non-overlapping expression of SR34 in cells of the growing root tip, however does suggest the existence of a distinct role for this SR protein (Lopato *et al.*, 1999). Another possibility for lack of phenotype is conditionality, which reflects the phenotypic plasticity and adaptive growth that plants exhibit to enhance their survival in changing conditions. In this investigation, a difference in root phenotype was seen when *sr34* mutants were grown on agar media supplemented with chemicals designed to mimic certain stresses that have been known to elicit conditional responses in other splicing factor mutants (Lee *et al.*, 2006; Palusa *et al.*, 2007; Duque, 2011; Huang *et al.*, 2013; Du *et al.*, 2015). These conditions included exposure to mannitol as an osmotic stress emulator, ABA as an inducer of stress responses, and added sucrose as a carbon source. Distinct differences in overall morphology were also seen in *sr34* mutants compared to WT when grown on heterogeneous media, perlite and peat, again indicating a sensitivity to, albeit less quantifiable, abiotic stress (e.g.

inconsistent carbon source, variation in water availability, etc.). These findings support a role for *SR34* in the regulation of ABA-mediated and ABA-independent stress responses, which corroborates previous work (Cruz *et al.*, 2014). Indeed, the ratios of different *SR34* splice isoforms has been noted to change with different conditions including exogenous ABA, as well as temperature and boric acid (Palusa *et al.*, 2007). Growth on media containing NaCl to simulate high salinity (osmotic and ionic stress) did not result in any significant difference in primary root length, a result that is consistent with previous findings that levels of functional *SR34* do not change upon exposure to this condition (Palusa *et al.*, 2007). The role that this link to stress responses plays in MDF signalling remains unclear.

4.3. CONCLUDING REMARKS

Structural homology, though limited, to other known spliceosome constituents and the presence of an RS domain common to splicing regulators provide evidence to support a function for MDF as a splicing factor. The significant differences in alternative splicing events in *mdf* mutants also lends credence to this claim. However, more evidence is required to demonstrate if MDF actually has a role in splicing regulation. Further investigation is necessary to decipher whether these alternative splicing events in mutants are a direct result of aberrant MDF splicing function, or rather a consequence of the stressful nature of the severe patterning defects seen in *mdf* mutants, as splicing is known to change under stress. Tissue-specific splicing events may also not be seen in *mdf* mutants due to the differences in the tissue and organs of mutants and WT plants. It is also still unclear if MDF interacts with other splicing-related factors. Mutants in genes mis-spliced in *mdf* mutants do not appear to phenocopy *mdf*, and many of the genes known to be regulated by MDF are not mis-spliced in mutants. If indeed it is a splicing factor, specifically how and where MDF would act to fine tune splicing and gene expression remains to be elucidated.

Further work would be required to address the interesting preliminary observations in this thesis and put them in the context of MDF signalling (Figure 4.2) and plant root development. An example of such work could include investigating the differential gene expression and alternative splicing of *SR34* specifically in the root tissue of *mdf* mutants and overexpressors, since hitherto only whole seedlings have been used. The significance

of *SR34* splice isoform dosage, and how MDF regulates this in response to different stimuli or developmental stages would also prove enlightening. While *sr34* mutants do not show complete phenocopying of *mdf* mutant root morphology, the reduction in root length suggests that *SR34* could play a role in root growth in response to certain abiotic stresses. Investigating the role of MDF in stress responses, especially in regards to root growth, through the regulation of *SR34* splice variants, would also provide an interesting avenue of research. Looking for hypersensitivity to abiotic stress in *mdf* mutants, and the effect of stress on *MDF* expression in WT may be a sensible starting point.

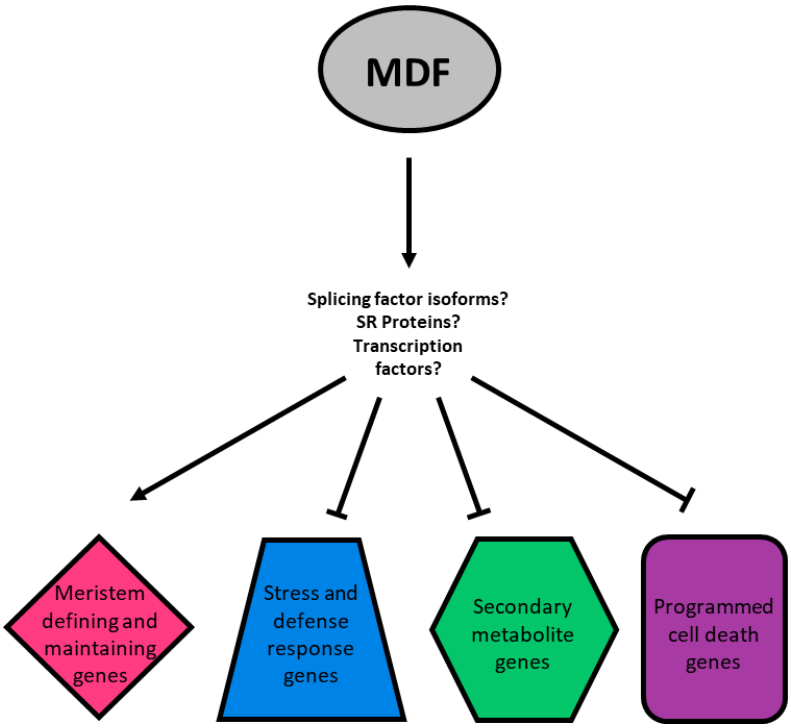

Figure 4.2. Proposed model of MDF signalling.

5. APPENDIX – PRIMER SEQUENCES

5.1. Testing Genomic DNA Contamination of cDNA

Table 5.1. Primer sequence for verifying the presence of genomic DNA in cDNA samples.

Associated Gene	AGI Locus Code	Forward Primer Sequence (5'→3')	Reverse Primer Sequence (5'→3')	Expected Band Sizes (bp)	PCR Annealing Temperature (°C)
ACT2	*AT3G18780*	GGATCGGTGGTTCCATTCTTGC	AGAGTTTGTCACACACAAGTGCA	cDNA = 256 gDNA = 342	55.2

5.2. NASC Line Genotyping PCR Primers

Table 5.2. Primer sequences for genotyping the presence of T-DNA insertions in plant lines purchased from NASC. An annealing temperature of 55 °C was used for all PCR reactions.

Associated Gene	AGI Locus Code	Left Primer Sequence (LP) (5'→3')	Right Primer Sequence (RP) (5'→3')	WT Band Sizes (bp)	Mutant Band Sizes (bp)
LBb1.3 SALK left border (LB)	-	ATTTTGCCGATTTCGGAAC	-	-	-
LB3 SAIL left border (LB)	-	TAGCATCTGAATTTCATAACCAATCTCGATACAC	-	-	-
sr33	*AT1G55310*	CTCCCCCTAGAAGACATCACC	TAGATTCGGTGGACGAGAATG	1035	473-773
sr34	*AT1G02840*	CATCTGCTTCTTGGCAAGATC	TCCAAGTGATCCAATGTCTCC	1246	610-910
sr45	*AT1G16610*	GGTCCATTTCTTGATCCTCAAG	GAACTGGAACGAGATGACGAG	1264	574-874
sr45a	*AT1G07350*	CACTGAGAACAACGGAGCTTC	CGAACCACAAAATCACAAAATC	1220	601-901
rsz33	*AT2G37340*	TGGATCATCCTTGCGTATCTC	GAGAGATCACGCAGTCCAAAG	1251	569-869
u2.2	*AT3G57645*	GAAGATCTCATCGAACGTTGC	AGAGCAGAAAAAGTTCCTCCG	1096	497-797
u2.4	*AT3G56825*	CAAAGATCGCTCAAGAAATGG	AGAGGCAAGCTTAATTAGGCG	1097	443-743
u2.6	*AT3G56705*	CCAAGAATCAGCCAACAAGAG	CGACAAGTTAGAGAGCGTTGG	1216	606-906
u5-3	*AT1G70185*	TGATCCGGTTTTAAAAATATTGG	CCTTCCAACAAGGTAGCAATG	1117	435-735
u6.29	*AT5G46315*	TTTGGTTATTCGAGGTGAAGG	TCATCTCGGTGGTAGAGTTCG	1180	575-875
u12	*AT1G61275*	AGTCACCATCGAATACATCGG	GGGTCCATCATCACTGAGATG	1223	558-858
ubp15	*AT1G17110*	TTTGGTTATTACCCAAAATGAGC	AATATTGGTATGTCCGCTCCC	1138	584-884

5.3. Gateway Cloning Primers

5.3.1. attB PCR Primers

Table 5.3. Primer sequences for generating *att*B-flanked PCR products from cDNA for Gateway cloning. Lower case indicates the *att*B-sites, and upper case denotes the sequence complementary to the gene of choice.

Associated Gene	AGI Locus Code	Forward Primer Sequence (5'→3')	Reverse Primer Sequence (5'→3')	Expected Band Size (bp)	PCR Annealing Temperature (°C)
MDF	*AT5G16780*	ggggacaagtttgtacaaaaaagcaggcttcgcaacaTCAAGGCTTTGGTCTCTTTG	ggggaccactttgtacaagaaagctgggtcAGGCTTTGGTCTCTTTG	2530	53.7
AGO4	*AT2G27040*	ggggacaagtttgtacaaaaaagcaggcttcgcaacaATGGATTCAACAAATGGTAACG	ggggaccactttgtacaagaaagctgggtcTTAACAGAAGAACATGGAGTTGG	2842	50.1
STA1	*AT4G03430*	ggggacaagtttgtacaaaaaagcaggcttcgcaacaATGGTGTTTCTCTCGATTCCAAAC	ggggaccactttgtacaagaaagctgggtcTCAAGCAGAATTCTCTTCCTTGCTC	3157	51.8
PRP38	*AT2G40650*	ggggacaagtttgtacaaaaaagcaggcttcgcaacaATGGCAAACAGAACAGATCCG	ggggaccactttgtacaagaaagctgggtcTCAGTCCCTGAGGGGTTTC	1135	53.7
PRP31	*AT1G60170*	ggggacaagtttgtacaaaaaagcaggcttcgcaacaATGGCAACTCTTGAAGATTCTTTC	ggggaccactttgtacaagaaagctgggtcTTAGATCTTCTTCAGCTTCGAGAAG	1525	Failed to amplify

5.3.2. DNA Sequencing Primers

Table 5.4. Consecutive primer sequences for the verification of entry clones produced via Gateway cloning. DNA sequencing was used to confirm the presence of the desired gene sequence. Each sequential primer was designed to be approximately 500 bp downstream of the previous one.

Associated Gene	Forward Primer Sequence (5'→3')
MDF	GGAAAAAGACAAGGATAGGGC
	CATGGTTTGGAGAAAGTGGTG
	GAGCAATGCCTATCAGGAAGCC
	AAAAAGAGCAAGCTTGTGGG
	TGGAAGCTTAACACCAATGC
AGO4	CATTCTGATCTGGATGGTAAAGA
	AACTGTGAACCAGTTGGTGG
	GATTTGCCTTGCATCAATGTT
	AATCAATTCCGCCGTGCTCC
	ACCATTATCCTTGGGATGGA
	AAGTTCTTCCAGCCAACGTC
STA1	TCGATCTGATATTGGTCCTGC
	GGAGGAGGTGGATGGGAAGATT
	CAAAGAATCCAAATGGCTGG
	GGCTCGAAACATATGCTGAA
	TGCTCTTAGTGTATTCTTGACCA
	AGGTTTGAAGCAATTCCCAA
	AGAAGTGTGATCGCGACCCT
PRP38	AAGCCTACTCCGTTCCTTTGCC
	ATGAAAGAGAACGTGGGCAT
PRP31	CAAGTACAAGCTTAAGTTTCAAGAGC
	TTTCTTCTGCAACGTCTCAGTCC
	AAGAGAGCTCCCTCGGTGAT

Associated Gene	Forward Primer Sequence (5'→3')	Reverse Primer Sequence (5'→3')
pDONR207	TCGCGTTAACGCTAGCATGGATCT	GTAACATCAGAGATTTTGAGACAC

5.3.3. Colony PCR Primers

Table 5.5. Primer sequences for verifying the expression of the desired Gateway constructs in *E. coli* colonies.

Associated Gene	Forward Primer Sequence (5'→3')	Reverse Primer Sequence (5'→3')	Expected Band Size of Positive Clones (bp)	PCR Annealing Temperature (°C)
MDF	GAGCAATGCCTATCAGGAAGCC	CTCCATCATCATCCACAATACCCAC	653	55.9
AGO4	AATCAATTCCGCCGTGCTCC	GCCATCGTCTTCAGTTCCATTTTTC	504	55.9
STA1	CGAGAAATACCGAGCCTCGAAC	AATCTTCCCATCCACCTCCTCC	535	55.9
PRP38	AAGCCTACTCCGTTCCTTTGCC	TCTGTCTCGTTCTCTATCTCTGCC	666	55.9
PRP31	TTTCTTCTGCAACGTCTCAGTCC	AGTCCCACTTCCTAATCCTAAAGCC	617	55.9

6. REFERENCES

Agafonov, D. E., Deckert, J., Wolf, E., Odenwälder, P., Bessonov, S., Will, C. L., Urlaub, H., & Lührmann, R. (2011). Semiquantitative Proteomic Analysis of the Human Spliceosome via a Novel Two-Dimensional Gel Electrophoresis Method. *Molecular and Cellular Biology, 31*(33), 2667-2682.

Arabidopsis Genome Initiative. (2000). Analysis of the genome sequence of the flowering plant *Arabidopsis thaliana*. *Nature, 408*(6814), 796-815.

Ausin, I., Greenberg, M. V., Li, C. F., & Jacobsen, S. E. (2012). The splicing factor SR45 affects the RNA-directed DNA methylation pathway in *Arabidopsis*. *Epigenetics, 7*(1), 29-33.

Beddington, J. (2010). Food security: contributions from science to a new and greener revolution. *Philosophical Transactions of the Royal Society B, 365*(1537), 61-71.

Beemster, G. T., & Baskin, T. I. (1998). Analysis of cell division and elongation underlying the developmental acceleration of root growth in *Arabidopsis thaliana*. *Plant Physiology, 116*(4), 1515-1526.

Bengough, A. G., McKenzie, B. M., Hallett, P. D., & Valentine, T. A. (2011). Root elongation, water stress, and mechanical impedance: a review of limiting stresses and beneficial root tip traits. *Journal of Experimental Botany, 62*(1), 59-68.

Bertram, K., Agafonov, D. E., Dybkov, O., Haselbach, D., Leelaram, M. N., Will, C. L., Urlaub, H., Kastner, B., Lührmann, R., & Stark, H. (2017). Cryo-EM Structure of a Pre-catalytic Human Spliceosome Primed for Activation. *Cell, 170*(4), 701-713.

Blanton, S., Srinviasan, A., & Rymond, B. C. (1992). PRP38 encodes a yeast protein required for pre-mRNA splicing and maintenance of stable U6 small nuclear RNA levels. *Molecular Cell Biology, 12*, 3939-3947.

Blilou, I., Xu, J., Wildwater, M., Willemsen, V., Paponov, I., Friml, J., Heidstra, R., Aida, M., Palme, K., & Scheres, B. (2005). The PIN auxin efflux facilitator network controls growth and patterning in *Arabidopsis* roots. *Nature, 433*(1), 39-44.

Boucher, L., Ouzounis, C. A., Enright, A. J., & Blencowe, B. J. (2001). A genome-wide survey of RS domain proteins. *RNA, 7*(12), 1693-1701.

Breitkreutz, B. J., Stark, C., & Tyers, M. (2003). The GRID: the General Repository for Interaction Datasets. *Genome Biology, 4*(3), R23.

Brückner, A., Polge, C., Lentze, N., Auerbach, D., & Schlattner, U. (2009). Yeast Two-Hybrid, a Powerful Tool for Systems Biology. *International Journal of Molecular Sciences, 10*(6), 2763–2788.

Burbulis, I. E., & Winkel-Shirley, B. (1999). Interactions among enzymes of the *Arabidopsis* flavonoid biosynthetic pathway. *Proceedings of the National Academy of Sciences of the United States of America, 96*(22), 12929-12934.

Cassiday, L. A., & Maher III, L. J. (2002). Having it both ways: transcription factors that bind DNA and RNA. *Nucleic Acids Research, 30*(19), 4118-4126.

Casson, S. A., & Lindsey, K. (2003). Genes and signalling in root development. *New Phytologist, 158*(1), 11-38.

Casson, S. A., Topping, J. F., & Lindsey, K. (2009). MERISTEM-DEFECTIVE, an RS domain protein, is required for the correct meristem patterning and function in *Arabidopsis*. *The Plant Journal, 57*(5), 857-869.

Casson, S., Spencer, M., Walker, K., & Lindsey, K. (2005). Laser capture microdissection for the analysis of gene expression during embryogenesis of *Arabidopsis*. *The Plant Journal, 42*(1), 111-123.

Chen, M., & Manley, J. L. (2009). Mechanisms of alternative splicing regulation: insights from molecular and genomics approaches. *Nature reviews Molecular cell biology, 10*(11), 741-754.

Clarke, M. C., Wei, W., & Lindsey, K. (1992). High-Frequency Transformation of *Arabidopsis thaliana* by *Agrobacterium tumefaciens*. *Plant Molecular Biology Reporter, 10*(2), 178-189.

Costanzo, M., VanderSluis, B., Koch, E. N., Baryshnikova, A., Pons, C., Tan, G., Wang, W., Usaj, M., Hanchard, J., Lee, S. D., Pelechano, V., Styles, E. B., Billmann, M., van Leeuwen, J., van Dyk, N., Lin, Z. Y., Kuzmin, E., Nelson, J., Piotrowski, J. S., Srikumar, T., Bahr, S., Chen, Y., Deshpande, R., Kurat, C. F., Li, S. C., Li, Z., Usaj, M. M., Okada, H., Pascoe, N., San Luis, B. J., Sharifpoor, S., Shuteriqi, E., Simpkins, S. W., Snider, J., Suresh, H. G., Tan, Y., Zhu, H., Malod-Dognin, N., Janjic, V., Przulj, N., Troyanskaya, O. G., Stagljar, I., Xia, T., Ohya, Y., Gingras, A. C., Raught, B., Boutros, M., Steinmetz, L. M., Moore, C. L., Rosebrock, A. P., Caudy, A. A., Myers, C. L., Andrews, B., & Boone, C. (2016). A global interaction network maps a wiring diagram of cellular function. *Science, 353*(6306), aaf1420.

Cruz, T. M., Carvalho, R. F., Richardson, D. N., & Duque, P. (2014). Abscisic Acid (ABA) Regulation of *Arabidopsis* SR Protein Gene Expression. *International Journal of Molecular Sciences, 15*(10), 17541-17564.

D'Andrea, L. D., & Regan, L. (2003). TPR proteins: the versatile helix. *Trends in Biochemical Sciences, 28*(12), 655-662.

Dolan, L., Janmaat, K., Willemsen, V., Linstead, P., Poethig, S., Roberts, K., & Scheres, B. (1993). Cellular organisation of the *Arabidopsis thaliana* root. *Development, 119*(7), 71-84.

Dou, K., Huang, C. F., Ma, Z. Y., Zhang, C. J., Zhou, J. X., Huang, H. W., Cai, T., Tang, K., Zhu, J. K., & He, X. J. (2013). The PRP6-like splicing factor STA1 is involved in RNA-directed DNA methylation by facilitating the production of Pol V-dependent scaffold RNAs. *Nucleic Acids Research, 41*(18), 8489-8502.

Du, J. L., Zhang, S. W., Huang, H. W., Cai, T., Li, L., Chen, S., & He, X. J. (2015). The Splicing Factor PRP31 Is Involved in Transcriptional Gene Silencing and Stress Response in *Arabidopsis*. *Molecular Plant, 8*(7), 1053-1068.

Duque, P. (2011). A role for SR proteins in plant stress responses. *Plant Signalling & Behaviour, 6*(1), 49-54.

Durfee, T., Becherer, K., Chen, P. L., Yeh, S. H., Yang, Y., Kilburn, A. E., Lee, W. H., & Elledge, S. J. (1993). The retinoblastoma protein associates with the protein phosphatase type 1 catalytic subunit. *Genes and Development, 7*(4), 555-569.

Edwards, K., Johnstone, C., & Thompson, C. (1991). A simple and rapid method for the preparation of plant genomic DNA for PCR analysis. *Nucleic Acids Research, 19*(6), 1349.

Ehlert, A., Weltmeier, F., Wang, X., Mayer, C. S., Smeekens, S., Vicente-Carbajosa, J., & Dröge-Laser, W. (2006). Two-hybrid protein–protein interaction analysis in *Arabidopsis* protoplasts: establishment of a heterodimerization map of group C and group S bZIP transcription factors. *The Plant Journal, 46*(5), 890-900.

Eun, C., Lorkovic, Z. J., Naumann, U., Long, Q., Havecker, E. R., Simon, S. A., Meyers, B. C., Matzke, A. J., & Matzke, M. (2011). AGO6 Functions in RNA-Mediated Transcriptional Gene Silencing in Shoot and Root Meristems in *Arabidopsis thaliana*. *PLoS One, 6*(10), e25730.

Galisson, F., & Legrain, P. (1993). The biochemical defects of prp4-1 and prp6-1 yeast splicing mutants reveal that the PRP6 protein is required for the accumulation of the [U4/U6.U5] tri-snRNP. *Nucleic Acids Research, 21*(7), 1555-1562.

Garcia-Blanco, M. A., Baraniak, A. P., & Lasda, E. L. (2004). Alternative splicing in disease and therapy. *Nature Biotechnology, 22*(5), 535-546.

Gavin, A. C., Aloy, P., Grandi, P., Krause, R., Boesche, M., Marzioch, M., Rau, C., Jensen, L. J., Bastuck, S., Dümpelfeld, B., Edelmann, A., Heurtier, M. A., Hoffman, V., Hoefert, C., Klein, K., Hudak, M., Michon, A. M., Schelder, M., Schirle, M., Remor, M., Rudi, T., Hooper, S., Bauer, A., Bouwmeester, T., Casari, G., Drewes, G., Neubauer, G., Rick, J. M., Kuster, B., Bork, P., Russell, R. B., & Superti-Furga, G. (2006). Proteome survey reveals modularity of the yeast cell machinery. *Nature, 440*(7084), 631-636.

Gavin, A. C., Bösche, M., Krause, R., Grandi, P., Marzioch, M., Bauer, A., Schultz, J., Rick, J. M., Michon, A. M., Cruciat, C. M., Remor, M., Höfert, C., Schelder, M., Brajenovic, M., Ruffner, H., Merino, A., Klein, K., Hudak, M., Dickson, D., Rudi, T., Gnau, V., Bauch, A., Bastuck, S., Huhse, B., Leutwein, C., Heurtier, M. A., Copley, R. R., Edelmann, A., Querfurth, E., Rybin, V., Drewes, G., Raida, M., Bouwmeester, T., Bork, P., Seraphin, B., Kuster, B., Neubauer, G., & Superti-Furga, G. (2002). Functional organization of the yeast proteome by systematic analysis of protein complexes. *Nature, 415*(6868), 141-147.

Gottschalk, A., Neubauer, G., Banroques, J., Mann, M., Lührmann, R., & Fabrizio, P. (1999). Identification by mass spectrometry and functional analysis of novel proteins of the yeast [U4/U6.U5] tri-snRNP. *The EMBO Journal, 18*(1), 4535-4548.

Gottschalk, A., Tang, J., Puig, O., Salgado, J., Neubauer, G., Colot, H. V., Mann, M., Séraphin, B., Rosbash, M., Lührmann, R., & Fabrizio, P. (1998). A comprehensive biochemical and genetic analysis of the yeast U1 snRNP reveals five novel proteins. *RNA, 4*(4), 374-393.

Graveley, B. R. (2000). Sorting out the complexity of SR protein functions. *RNA, 6*(1), 1197–1211.

Gupta, M., Mungai, P. T., & Goldwasser, E. (2000). A newtransacting factor that modulates hypoxia-induced expression of the erythropoietin gene. *Blood, 96*(2), 491-497.

Häcker, I., Sander, B., Golas, M. M., Wolf, E., Karagöz, E., Kastner, B., Stark, H., Fabrizio, P., & Lührmann , R. (2008). Localization of Prp8, Brr2, Snu114 and U4/U6 proteins in the yeast tri-snRNP by electron microscopy. *Nature Structural & Molecular Biology, 15*(11), 1206–1212.

Hall, S. L., & Padgett, R. A. (1994). Conserved sequences in a class of rare eukaryotic nuclear introns with non-consensus splice sites. *Journal of Molecular Biology, 239*(3), 357-365.

Hall, S. L., & Padgett, R. A. (1996). Requirement of U12 snRNA for in vivo splicing of a minor class of eukaryotic nuclear pre-mRNA introns. *Science, 271*(5256), 1716-1718.

Hartley, J. L., Temple, G. F., & Brasch, M. A. (2000). DNA Cloning Using in vitro Site-Specific Recombination. *Genome Research, 10*, 1788-1795.

Havecker, E. R., Wallbridge, L. M., Hardcastle, T. J., Bush, M. S., Kelly, K. A., Dunn, R. M., Schwach, F., Doonan, J. H., & Baulcombe, D. C. (2010). The *Arabidopsis* RNA-directed DNA methylation argonautes functionally diverge based on their expression and interaction with target loci. *Plant Cell, 22*(2), 321-334.

Havugimana, P. C., Hart, G. T., Nepusz, T., Yang, H., Turinsky, A. L., Li, Z., Wang, P. I., Boutz, D. R., Fong, V., Phanse, S., Babu, M., Craig, S. A., Hu, P., Wan, C., Vlasblom, J., Dar, V. U., Bezginov, A., Clark, G. W., Wu, G. C., Wodak, S. J., Tillier, E. R., Paccanaro, A., Marcotte, E. M., & Emili, A. (2012). A census of human soluble protein complexes. *Cell, 150*(5), 1068-1081.

Hawkins, T. J. (2004). A study of M0R1/GEM1 and kinl-like kinesins in *Arabidopsis*. *Durham theses, Durham University. Available at Durham E-Theses Online: http://etheses.dur.ac.uk/3039/*.

Hein, M. Y., Hubner, N. C., Poser, I., Cox, J., Nagaraj, N., Toyoda, Y., Gak, I. A., Weisswange, I., Mansfeld, J., Buchholz, F., Hyman, A. A., & Mann, M. (2015). A Human Interactome in Three Quantitative Dimensions Organized by Stoichiometries and Abundances. *Cell, 3*(22), 712-723.

Hetherington, F. M. (2018). The response of *Arabidopsis* to low potassium availability. *Durham theses, Durham University. Available at Durham E-Theses Online: http://etheses.dur.ac.uk/12457/*.

Hosokawa, M., Kadota, R., Shichijo, S., Itoh, K., Dmitriev, I., Krasnykh, V., Curiel, D. T., Takue, Y., Wakasugi, H., Takashima, S., & Heike, Y. (2005). Cell cycle arrest and apoptosis induced by SART-1 gene transduction. *Anticancer research, 35*(3B), 1983-1990.

Huang, C. F., & Zhu, J. K. (2014). RNA Splicing Factors and RNA-Directed DNA Methylation. *Biology, 3*(2), 243-254.

Huang, C. F., Miki, D., Tang, K., Zhou, H. R., Zheng, Z., Chen, W., Ma, Z. Y., Yang, L., Zhang, H. Liu, R., He, X. J., & Zhu, J. K. (2013). A Pre-mRNA-splicing factor is required for RNA-directed DNA methylation in *Arabidopsis*. *PLoS Genetics, 9*(9), e1003779.

Iyer-Pascuzzi, A. S., Jackson, T., Cui, H., Petricka, J., Busch, W., Tsukagoshi, H., & Benfey, P. N. (2011). Cell Identity Regulators Link Development and Stress Responses in the *Arabidopsis* Root. *Developmental Cell, 21*(4), 770-782.

Jackson, I. J. (1991). A reappraisal of non-consensus mRNA splice sites. *Nucleic Acids Research, 19*(14), 3795-3798.

Kalyna, M., & Barta, A. (2004). A plethora of plant serine/arginine-rich proteins: redundancy or evolution of novel gene functions? *Biochemical society transactions, 32*(4), 561-564.

Kanehisa, M., & Goto, S. (2000). Kyoto Encyclopedia of Genes and Genomes. *Nucleic Acid Research, 28*(1), 27-30.

Kelemen, O., Convertini, P., Zhang, Z., Wen, Y., Shen, M., Falaleeva, M., & Stamm, S. (2013). Function of alternative splicing. *Gene, 514*(1), 1-30.

Kolossova, I., & Padgett, R. A. (1997). U11 snRNA interacts in vivo with the 5' splice site of U12-dependent (AU-AC) pre-mRNA introns. *RNA, 3*(3), 227-233.

Koncz, C., Chua, N. H., & Schell, J. (Eds.). (1992). *Methods in Arabidopsis research.* World Scientific Publishing Company.

Krogan, N. J., Cagney, G., Yu, H., Zhong, G., Guo, X., Ignatchenko, A., Li, J., Pu, S., Datta, N., Tikuisis, A. P., Punna, T., Peregrín-Alvarez, J. M., Shales, M., Zhang, X., Davey, M., Robinson, M. D., Paccanaro, A., Bray, J. E., Sheung, A., Beattie, B., Richards, D. P., Canadien, V., Lalev, A., Mena, F., Wong, P., Starostine, A., Canete, M. M., Vlasblom, J., Wu, S., Orsi, C., Collins, S. R., Chandran, S., Haw, R., Rilstone, J. J., Gandi, K., Thompson, N. J., Musso, G., St Onge, P., Ghanny, S., Lam, M. H., Butland, G. , Altaf-Ul, A. M., Kanaya, S., Shilatifard, A., O'Shea, E., Weissman, J. S., Ingles, C. J., Hughes, T. R., Parkinson, J., Gerstein, M., Wodak, S. J., Emili, A., & Greenblatt, J. F. (2006). Global landscape of protein complexes in the yeast *Saccharomyces cerevisiae*. *Nature, 440*(7084), 637-643.

Laibach, F. (1943). *Arabidopsis thaliana* (L.) Heynh. als Objekt für genetische und entwicklungsphysiologische Untersuchungen. *Bot. Archiv, 44*, 439-455.

Lee, B. H., Kapoor, A., Zhu, J., & Zhu, J. K. (2006). STABILIZED1, a stress-upregulated nuclear protein, is required for pre-mRNA splicing, mRNA turnover, and stress tolerance in *Arabidopsis*. *Plant Cell, 18*(7), 1736-1749.

Lee, J. H., Ryu, H. S., Chung, K. S., Posé, D., Kim, S., Schmid, M., & Ahn, J. H. (2013). Regulation of temperature-responsive flowering by MADS-box transcription factor repressors. *Science, 342*(6158), 628-632.

Lee, S. A., Chan, C. H., Tsai, C. H., Lai, J. M., Wang, F. S., Kao, C. Y., & Huang, C. F. (2008). Ortholog-based protein-protein interaction prediction and its application to inter-species interactions. *BMC Bioinformatics, 9*(12), S11.

Li, X., Wang, W., Wang, J., Malovannaya, A., Xi, Y., Li, W., Guerra, R., Hawke, D. H., Qin, J., & Chen, J. (2015). Proteomic analyses reveal distinct chromatin-associated and soluble transcription factor complexes. *Molecular Systems Biology, 11*, 775.

Lindsey, K., & Topping, J. F. (1993). Embryogenesis: a Question of Pattern. *Journal of Experimental Botany, 44*(2), 359-374.

Liu, J., Rowe, J., & Lindsey, K. (2014). Hormonal crosstalk for root development: a combined experimental and modeling perspective. *Frontiers in Plant Science, 5*.

Liu, J., Sun, N., Liu, J., Du, B., Wang, X., & Qi, X. (2013). An autoregulatory loop controlling *Arabidopsis* HsfA2 expression: role of heat shock-induced alternative splicing. *Plant Physiology, 162*(1), 512-521.

Liu, S., Li, P., Nottrott, S., Hartmuth, K., Lührmann, R., Carlomagno , T., & Wahl, M. C. (2007). Binding of the human Prp31 Nop domain to a composite RNA-protein platform in U4 snRNP. *Science, 6*(316), 115-120.

Liu, S., Rauhut, R., Vornlocher, H. P., & Lührmann, R. (2006). The network of protein–protein interactions within the human U4/U6.U5 tri-snRNP. *RNA, 12*(1), 1418-1430.

Lopato, S., Kalyna, M., Dorner, S., Kobayashi, R., Krainer, A. R., & Barta, A. (1999). atSRp30, one of two SF2/ASF-like proteins from *Arabidopsis thaliana*, regulates splicing of specific plant genes. *Genes & Development, 13*(8), 987-1001.

Lopato, S., Mayeda, A., Krainer, A. R., & Barta, A. (1996). Pre-mRNA splicing in plants: characterization of Ser/Arg splicing factors. *Proceedings of the National Academy of Sciences of the United States of America, 93*(7), 3074-3079.

López-Bucio, J., Cruz-Ramírez, A., & Herrera-Est, L. (2003). The role of nutrient availability in regulating root architecture. *Current Opinion in Plant Biology, 6*(3), 280-287.

Lorković, Z. J., & Barta, A. (2002). Genome analysis: RNA recognition motif (RRM) and K homology (KH) domain RNA-binding proteins from the flowering plant *Arabidopsis thaliana*. *Nucleic Acids Research, 30*(3), 623-635.

Lorkovic, Z. J., Lehner, R., Forstner, C., & Barta, A. (2005). Evolutionary conservation of minor U12-type spliceosome between plants and humans. *RNA, 11*(7), 1095-1107.

Makarov, E. M., Makarova, O. V., Achsel, T., & Lührmann, R. (2000). The human homologue of the yeast splicing factor prp6p contains multiple TPR elements and is stably associated with the U5 snRNP via protein-protein interactions. *Journal of Molecular Biology, 298*(4), 567-575.

Makarov, E., Makarova, O., Urlaub, H., Gentzel, M., Will, C., Wilm, M., & Lührmann, R. (2002). Small nuclear ribonucleoprotein remodeling during catalytic activation of the spliceosome. *Science, 298*(5601), 2205-2208.

Makarova, O. V., Makarov, E. M., Liu, S., Vornlocher, H. P., & Lührmann, R. (2002). Protein 61K, encoded by a gene (PRPF31) linked to autosomal dominant retinitis pigmentosa, is required for U4/U6·U5 tri-snRNP formation and pre-mRNA splicing. *The EMBO Journal, 21*(5), 1148–1157.

Makarova, O. V., Makarov, E. M., & Lührmann, R. (2001). The 65 and 110 kDa SR-related proteins of the U4/U6.U5 tri-snRNP are essential for the assembly of mature spliceosomes. *The EMBO Journal, 20*(10), 2553-2563.

Martínez-Zapater, J. M., & Salinas, J. (Eds.). (1998). *Arabidopsis Protocols.* Methods in Molecular Biology.

McGlincy, N. J., & Smith, C. W. (2008). Alternative splicing resulting in nonsense-mediated mRNA decay: what is the meaning of nonsense? *Trends in biochemical sciences, 33*(8), 385-393.

Meyerowitz, E. M. (1989). *Arabidopsis*, a useful weed. *Cell, 56*(2), 263-269.

Mishra, S. K., Ammon, T., Popowicz, G. M., Krajewski, M., Nagel, R. J., Ares, M., Holak, T. A., & Jentsch, S. (2011). Role of the ubiquitin-like protein Hub1 in splice-site usage and alternative splicing. *Nature, 474*(7350), 173.

Murashige, T., & Skoog, F. (2006). A Revised Medium for Rapid Growth and Bio Assays with Tobacco Tissue Cultures. *Physiologia Plantarum , 15*(3), 473-497.

Nguyen, P. V., Srihari, S., & Leong, H. W. (2013). Identifying conserved protein complexes between species by constructing interolog networks. *BMC bioinformatics, 14*(16), S8.

Nottrott, S., Urlaub, H., & Lührmann, R. (2002). Hierarchical, clustered protein interactions with U4/U6 snRNA: a biochemical role for U4/U6 proteins. *The EMBO Journal, 21*(20), 5527-5538.

Osborne, M. A., Dalton, S., & Kochan, J. P. (1995). The yeast tribrid system - genetic detection of trans-phosphorylated ITAM-SH2-interactions. *Bio/Technology, 13*(12), 1474.

Osborne, M. A., Zenner, G., Lubinus, M., Zhang, X., Songyang, Z., Cantley, L. C., Majerus, P., Burn, P., & Kochan, J. P. (1996). The Inositol 5'-Phosphatase SHIP Binds to Immunoreceptor Signaling Motifs and Responds to High Affinity IgE Receptor Aggregation. *The Journal of Biological Chemistry, 271*(46), 29271-29278.

Palusa, S. G., Ali, G. S., & Reddy, A. S. (2007). Alternative splicing of pre-mRNAs of *Arabidopsis* serine/arginine-rich proteins: regulation by hormones and stresses. *The Plant Journal, 49*(6), 1091-1107.

Peterson, R. L. (1992). Adaptations of root structure in relation to biotic and abiotic factors. *Canadian Journal of Botany, 70*(4), 661-675.

Petricka, J. J., Clay, N. K., & Nelson, T. M. (2008). Vein patterning screens and the defectively organized tributaries mutants in *Arabidopsis thaliana*. *The Plant Journal, 56*(2), 251–263.

Petricka, J. J., Winter, C. M., & Benfey, P. N. (2012). Control of *Arabidopsis* Root Development. *Annual Review of Plant Biology, 63*, 563-590.

Plaschka, C., Lin, P. C., & Nagai, K. (2017). Structure of a pre-catalytic spliceosome. *Nature, 546*(7660), 617-621.

Posé, D., Verhage, L., Ott, F., Yant, L., Mathieu, J., Angenent, G. C., Immink, R. G. H., & Schmid, M. (2013). Temperature-dependent regulation of flowering by antagonistic FLM variants. *Nature*, 414-417.

Qi, Y., He, X., Wang, X. J., Kohany, O., Jurka, J., & Hannon, G. J. (2006). Distinct catalytic and noncatalytic roles of ARGONAUTE4 in RNA-directed DNA methylation. *Nature, 443*(7114), 1008-1012.

Rajagopala, S. V., & Uetz, P. (2009). Analysis of Protein–Protein Interactions Using Array-Based Yeast Two-Hybrid Screens. *Yeast Functional Genomics and Proteomics, 548*, 223-245.

Reddy, A. S., & Shad Ali, G. (2011). Plant serine/arginine-rich proteins: roles in precursor messenger RNA splicing, plant development, and stress responses. *Wiley Interdisciplinary Reviews, 2*(6), 875-889.

Reddy, A. S., Marquez, Y., Kalyna, M., & Barta, A. (2013). Complexity of the Alternative Splicing Landscape in PlantsC. *The Plant Cell, 25*(1), 3657-3683.

Richardson, D. N., Rogers, M. F., Labadorf, A., Ben-Hur, A., Guo, H., Paterson, A. H., & Reddy, A. S. (2011). Comparative Analysis of Serine/Arginine-Rich Proteins across 27 Eukaryotes: Insights into Sub-Family Classification and Extent of Alternative Splicing. *PLoS One, 6*(9), e24542.

Robinson, D. (1994). The responses of plants to non-uniform supplies of nutrients. *New Phytologist, 127*(4), 635-674.

Sanz, L., Murray, J. A., & Dewitte, W. (2012). To divide and to rule; regulating cell division in roots during post-embryonic growth. *Progress in Botany, 73*, 57-80.

Schaffert, N., Hossbach, M., Heintzmann, R., Achsel, T., & Lührmann, R. (2004). RNAi knockdown of hPrp31 leads to an accumulation of U4/U6 di-snRNPs in Cajal bodies. *The EMBO Journal, 23*(15), 3000-3009.

Scheufler, C., Brinker, A., Bourenkov, G., Pegoraro, S., Moroder, L., Bartunik, H., Hartl, F. U., & Moarefi, I. (2000). Structure of TPR domain-peptide complexes: critical elements in the assembly of the Hsp70-Hsp90 multichaperone machine. *Cell, 101*(2), 199-210.

Schneider, C. A., Rasband, W. S., & Eliceiri, K. W. (2012). NIH Image to ImageJ: 25 years of image analysis. *Nature Methods, 9*, 671-675.

Schneider, M., Hsiao, H. H., Giet, R., Urlaub, H., & Lührmann, R. (2010). Human PRP4 kinase is required for stable tri-snRNP association during spliceosomal B complex formation. *Nature Structural & Molecular Biology, 17*(2), 216-221.

Schoof, H. L., Haecker, A., Mayer, K., Jurgens, G., & Laux, T. (2000). The stem cell population of *Arabidopsis* shoot meristems is maintained by a regulatory loop between the CLAVATA and WUSCHEL genes. *Cell, 100*(1), 635-644.

Schütze, T., Ulrich, A. K., Apelt, L., Will, C. L., Bartlick, N., Seeger, M., Weber, G., Lührmann, R., Stelzl, U., & Wahl, M. C. (2016). Multiple protein–protein interactions converging on the Prp38 protein during activation of the human spliceosome. *RNA, 22*(2), 265-277.

Seo, P. J., Park, M. J., Lim, M. H., Kim, S. G., Lee, M., Baldwin, I. T., & Park, C. M. (2012). A self-regulatory circuit of CIRCADIAN CLOCK-ASSOCIATED1 underlies the circadian clock regulation of temperature responses in *Arabidopsis*. *Plant Cell, 24*(6), 2427-2442.

Shad Ali, G., Palusa, S. G., Golovkin, M., Prasad, J., Manley, J. L., & Reddy, A. S. (2007). Regulation of Plant Developmental Processes by a Novel Splicing Factor. *PLoS One*, e471.

Shen, W. (2018). Genetic Control of Root Development in *Arabidopsis*. *Durham theses, Durham University*.

Simillion, C., Vandepoele, K., Van Montagu, M. C., Zabeau, M., & Van de Peer, Y. (2002). The hidden duplication past of *Arabidopsis thaliana*. *Proceedings of the National Academy of Sciences of the United States of America, 99*(21), 13627-13632.

Stahl, Y., & Simon, R. (2005). Plant stem cell niches. *The International Journal of Developmental Biology, 49*(5-6), 479-489.

Staiger, D., & Brown, J. W. (2013). Alternative splicing at the intersection of biological timing, development, and stress responses. *Plant Cell, 25*(10), 3640-3656.

Stamm, S., Ben-Ari, S., Rafalska, I., Tang, Y., Zhang, Z., Toiber, D., Thanaraj, T. A. & Soreq, H. (2005). Function of alternative splicing. *Gene*(344), 1-20.

Stankovic, N., Schloesser, M., Joris, M., Sauvage, E., Hanikenne, M., & Motte, P. (2016). Dynamic distribution and interaction of the *Arabidopsis* SRSF1 subfamily splicing factors. *Plant physiology, 170*(2), 1000-1013.

Stevens, S. W., & Abelson, J. (1999). Purification of the yeast U4/U6.U5 small nuclear ribonucleoprotein particle and identification of its proteins. *Proceedings of the National Academy of Sciences of the United States of America, 96*(13), 7226–7231.

Stevens, S. W., Barta, I., Ge, H. Y., Moore, R. E., Young, M. K., Lee, T. D., & Abelson, J. (2001). Biochemical and genetic analyses of the U5, U6, and U4/U6 x U5 small nuclear ribonucleoproteins from *Saccharomyces cerevisiae*. *RNA, 7*(11), 1543-1553.

Tacke, R., & Manley, J. L. (1999). Determinants of SR protein specificity. *Current Opinion in Cell Biology, 11*(1), 358-362.

Tarn, W. Y., & Steitz, J. A. (1996). Highly diverged U4 and U6 small nuclear RNAs required for splicing rare AT-AC introns. *Science, 273*(5283), 1824-1832.

Thompson, H. (2018). Personal Communication. *Durham University*.

Torres, M. A., Dangl, J. L., Dangl, J. L., & Jones, J. D. (2002). *Arabidopsis* gp91phox homologues AtrbohD and AtrbohF are required for accumulation of reactive oxygen intermediates in the plant defense response. *Proceedings of the National Academy of Sciences of the United States of America, 99*(1), 517-522.

Ubeda-Tomás, S., Beemster, G. S., & Bennett, M. J. (2012). Hormonal regulation of root growth: integrating local activities into global behaviour. *Trends in Plant Science, 17*(6), 326-331.

van Aelst, L., Barr, M., Marcus, S., Polverino, A., & Wigler, M. (1993). Complex formation between RAS and RAF and other protein kinases. *Proceedings of the National Academy of Sciences of the United States of America, 90*(13), 6213-6217.

van den Berg, C., Weisbeek, P., & Scheres, B. (1998). Cell fate and cell differentiation status in the *Arabidopsis* root. *Planta, 205*(4), 481-491.

van den Berg, C., Willemsen, V., Hendriks, G., & Scheres, B. (1997). Short-range control of cell differentiation in the *Arabidopsis* root meristem. *Nature, 390*(6657), 287-289.

van Nues, R. W., & Beggs, J. D. (2001). Functional Contacts With a Range of Splicing Proteins Suggest a Central Role for Brr2p in the Dynamic Control of the Order of Events in Spliceosomes of *Saccharomyces cerevisiae*. *Genetics, 157*(4), 1451-1467.

Vanstraelen, M., & Benková, E. (2012). Hormonal interactions in the regulation of plant development. *Annual Review of Cell and Developmental Biology, 28*(1), 463-487.

Varjosalo, M., Keskitalo, S., Van Drogen, A., Nurkkala, H., Vichalkovski, A., Aebersold, R., & Gstaiger, M. (2013). The Protein Interaction Landscape of the Human CMGC Kinase Group. *Cell Reports, 3*(4), 1306-1320.

Verbelen, J. P., De Cnodder, T., Le, J., Vissenberg, K., & Baluska, F. (2006). The Root Apex of *Arabidopsis thaliana* Consists of Four Distinct Zones of Growth Activities: Meristematic Zone, Transition Zone, Fast Elongation Zone and Growth Terminating Zon. *Plant Signalling & Behaviour, 1*(6), 296-304.

Vignols, F., Bréhélin, C., Surdin-Kerjan, Y., Thomas, D., & Meyer, Y. (2005). A yeast two-hybrid knockout strain to explore thioredoxin-interacting proteins in vivo. *Proceedings of the National Academy of Sciences of the United States of America, 102*(46), 16729-16734.

von Mering, C., Huynen, M., Jaeggi, D., Schmidt, S., Bork, P., & Snel, B. (2005). STRING: a database of predicted functional associations between proteins. *Nucleic Acids Research, 1*(33), D433-7.

Kagan, O., Kwan, J., Bezginov, A., Chessman, K., Pal, S., Cromar, G., Papoulas, O., Ni, Z., Boutz, D. R., Stoilova, S., Havugimana, P. C., Guo, X., Malty, R. H., Sarov, M., Greenblatt, J., Babu, M., Derry, W. B., Tillier, E. R., Wallingford, J. B., Parkinson, J., Marcotte, E. M., & Emili, A. (2015). Panorama of ancient metazoan macromolecular complexes. *Nature, 525*(7569), 339-344.

Wang, B. B., & Brendel, V. (2004). The ASRG database: identification and survey of *Arabidopsis* thalianagenes involved in pre-mRNA splicing. *Genome Biology, 5*(12), R102.

Weidenhammer, E. M., Ruiz-Noriega, M., & Woolford, J. L. (1997). Prp31p promotes the association of the U4/U6·U5 tri-snRNP with prespliceosomes to form spliceosomes in *Saccharomyces cerevisiae*. *Molecular and Cellular Biology, 17*(7), 3580–3588.

Weidenhammer, E. M., Singh, M., Ruiz-Noriega, M., & Woolford, J. L. (1996). The PRP31 gene encodes a novel protein required for Pre-mRNA splicing in *Saccharomyces cerevisiae*. *Nucleic Acids Research, 24*(6), 1164-1170.

Wheatley, A. P., Bolland, D. J., Hewitt, J. E., Dewar, J. C., & Hall, I. P. (2002). Identification of the autoantigen SART-1 as a candidate gene for the development of atop. *Human molecular genetics, 11*(18), 2143-2146.

Wilkinson, C. R., Dittmar, G. A., Ohi, M. D., Uetz, P., Jones, N., & Finley, D. (2004). Ubiquitin-like Protein Hub1 Is Required for Pre-mRNA Splicing and Localization of an Essential Splicing Factor in Fission Yeast. *Current Biology, 14*(24), 2283-2288.

Winter, D., Vinegar, B., Nahal, H., Ammar, R., Wilson, G. V., & Provart, N. J. (2007). An "Electronic Fluorescent Pictograph" Browser for Exploring and Analyzing Large-Scale Biological Data Sets. *PLoS One, 2*(8), e718.

Wu, J. Y., & Maniatis, T. (1993). Specific interactions between proteins implicated in splice site selection and regulated alternative splicing. *Cell, 75*(1), 1061-10700.

Xie, J., Beickman, K., Otte, E., & Rymond, B. C. (1998). Progression through the spliceosome cycle requires Prp38p function for U4/U6 snRNA dissociation. *The EMBO Journal, 17*(10), 2938-2946.

Yan, Q., Xia, X., Sun, Z., & Fang, Y. (2017). Depletion of *Arabidopsis* SC35 and SC35-like serine/arginine-rich proteins affects the transcription and splicing of a subset of genes. *PLoS Genetics, 13*(3), e1006663.

Zhang, C. J., Zhou, J. X., Liu, J., Ma, Z. Y., Zhang, S. W., Dou, K., Huang, H. W., Cai, T., Liu, R., Zhu, J. K., & He, X. J. (2013). The splicing machinery promotes RNA-directed DNA methylation and transcriptional silencing in *Arabidopsis*. *The EMBO Journal*, 1128-1140.

Zhang, W., Du, B., Liu, D., & Qi, X. (2014). Splicing factor SR34b mutation reduces cadmium tolerance in *Arabidopsis* by regulating iron-regulated transporter 1 gene. *Biochemical and Biophysical Research Communications, 455*(3-4), 312-317.

Zhang, X. C., & Gassmann, W. (2003). RPS4-mediated disease resistance requires the combined presence of RPS4 transcripts with full-length and truncated open reading frames. *Plant Cell*, 2333-2342.

Zheng, X., Zhu, J., Kapoor, A., & Zhu, J. K. (2007). Role of *Arabidopsis* AGO6 in siRNA accumulation, DNA methylation and transcriptional gene silencing. *The EMBO Journal, 26*(6), 1691-1701.

Zilberman, D., Cao, X., & Jacobsen, S. E. (2003). ARGONAUTE4 control of locus-specific siRNA accumulation and DNA and histone methylation. *Science, 299*(5607), 716-719.

Zilberman, D., Cao, X., Johansen, L. K., Xie, Z., Carrington, J. C., & Jacobsen, S. E. (2004). Role of *Arabidopsis* ARGONAUTE4 in RNA-directed DNA methylation triggered by inverted repeats. *Current Biology, 14*(13), 1214-1220.

Zimmermann, P., Hirsch-Hoffmann, M., Hennig, L., & Gruissem, W. (2004). GENEVESTIGATOR. Arabidopsis Microarray Database and Analysis Toolbox. *Plant Physiology, 136*, 2621-2632.